IJPSR (2022), Volume 13, Issue 9 (Research Article)

INTERNATIONAL JOURNAL OF PHARMACEUTICAL SCIENCES AND RESEARCH

Received on 04 January 2022; received in revised form, 07 March 2022; accepted 26 April 2022; published 01 September 2022

IN-SILICO ASSESSMENT *VIA* MOLECULAR DOCKING AND ADMET PROFILE OF BOTANICAL DRUGS (BERGAMOTTIN AND CASTICIN) AGAINST TRIAL DRUGS FOR LASSA VIRUS

Ibrahim Asiata Omotayo [1], Adepoju Adewusi John [1], Olafare Oluwafemi Gbenga [1], Abdul-Hammed Misbaudeen [1], Latona Dayo Felix [2], Oyebamiji Abel Kolawole [3] and Semire Banjo [*1]

Department of Pure and Applied Chemistry [1], Ladoke Akintola University of Technology, P.M.B. 4000, Ogbomoso, Oyo-State, Nigeria.
Department of Pure and Applied Chemistry [2], Osun State University, Osogbo, Nigeria.
Department of Basic Sciences [3], Adeleke University, P. M. B. 250, Ede, Osun State, Nigeria.

Keywords:

Lassa fever, Botanical drugs, Remdesvir, Molecular docking, ADMET

Correspondence to Author:
Semire Banjo

Department of Pure and Applied Chemistry, Ladoke Akintola University of Technology, P.M.B. 4000, Ogbomoso, Oyo-State, Nigeria.

E-mail: bsemire@lauctech.edu.ng

ABSTRACT: Lassa fever is a serious viral haemorrhagic illness caused by Lassa virus, a family of Arenaviridae. This haemorrhagic fever has become rampant in West Africa especially in Sierra Leone, the Republic of Guinea, Liberia and Nigeria, through exposure to food or household items contaminated with urine or faeces of infected Mastomys rats. There has been no vaccines or particular antiviral agents/drugs against the treatment of Lassa fever, but some drugs such ribavirin, lacidipine, phenothrin and remdesvir are being used in the early stage of the illness. The goal of the present work was to use *in-silico* methods via molecular docking and ADMET properties to assess the effectiveness of these drugs alongside the botanical drugs (Bergamottin and Casticin) found in grapefruits and *Artemisia annua.* The results showed that Remdesvir possesses outstanding inhibitory action against nucleoprotein (NP) of the Lassa virus, although Phenothrin and Casticin were active against 3MWP, Lacidipine and Casticin were active against 3MWT, 3MX5 and 3T5Q and Bergamottin, and Casticin were against 3T5N and 4FVU; Thus Remdesvir and Casticin (a botanical drug) could be used satisfactorily for the treatment of lassa fever.

INTRODUCTION: *Mastomys natalensis*, a peridomestic multimammate rodent, is a natural reservoir of Lassa fever virus. Mastomys rodents are well distributed throughout the sub-Saharan West Africa [1]. It has been reported that *Hylomyscus pamfi* and *Mastomys erthrocyclus* species are major reservoirs, as well as carriers of lassa virus.

QUICK RESPONSE CODE

DOI: 10.13040/IJPSR.0975-8232.13(9).3494-18

This article can be accessed online on www.ijpsr.com

DOI link: http://dx.doi.org/10.13040/IJPSR.0975-8232.13(9).3494-18

This virus from Mastomys finds its way into humans through direct contact with rodent excreta, rodent bites, rodent urine, as well as through handling and eating of rodents; these are common in rural areas in West African countries [2, 3]. *Lassa virus* belongs to a family of Arenaviridae, a genus Mammarena virus.

The hemorrhagic fever has become rampant in West Africa especially in Sierra Leone, the Republic of Guinea, Liberia and Nigeria [4, 5], this fever gets to its peak in the dry seasons. The Nigeria Centre reported for Disease Control that in 2020, over 4,761 suspected cases were reported, with about 15-20% of the cases developed into active hemorrhagic fever by 17th May, 2020 [6]. The

overall rate of fatality has been estimated to be 1%; however, the mortality rate can be as high as 50% during epidemics [7]. The period of incubation of Lassa fever is between six to twenty-one days after infection, and its symptoms similar to that of typhoid fever and malaria. The early symptoms include weakness, sore throat, body pains, malaise, fever, nausea, diarrhea, vomiting, and cough [8, 9], while the later stage symptoms include mucosal and internal bleeding, seizures, disorientation, coma and deafness [8]. Till date, there is no vaccines or particular antiviral agents/drugs against the treatment of Lassa fever; however, therapeutic approaches are limited to the administration of ribavirin in the early stage of the illness. Others drugs such as Lacidipine, Phenothrine and Remdesvir have been identified as entry inhibitors of lassa virus by blocking low-pH-induced membrane fusion [10].

More recently, the use of medicinal plants extracts for the treatment of virus-related diseases are now being recognized as a result of prevalence in drug-resistant virus diseases; therefore, more of plant extracts are now being tested against the resistant strain. Bergamottin and Casticin are two compounds found in grapefruits and *Artemisia annua* respectively; these compounds have been found to be active against lassa virus. Bergamottin, known as 5-geranoxypsoralen, is a natural furanocoumarin found in the pomelos pulp, peel and pulp of the bergamot orange [11], whereas, Casticin is a methyoxylated flavonol, also found in *Vitex agnus* [12,13].

Casticin has inhibited LASV entry by blocking low-pH-induced membrane fusion, F446L mutation, located in the transmembrane domain of GP2 is resistance to casticin [14-16]. However, bergamottin has shown to slightly affect LASV GPC-mediated membrane fusion, inhibiting LASV entry by blocking endocytic trafficking [14, 17-19]. Remarkably, both bergamottin and casticin have been reported to show inhibitory effects on authentic lymphocytic choriomeningitis virus [14]. However, in this present work, *in-silico* methods were used to assess the potency and safety of Bergamottin and Casticin; the two botanical drugs *via* molecular docking and ADMET profiling. The results were compared with four commercial drugs (Lacidipine, Phenothrine, Remdesvir and Ribavirin) that are being used for the treatment of patients with Lassa fever, these drugs are were docked against nucleoprotein (NP) of the Lassa virus; 3MWP, 3MWT, 3MX2, 3MX5, 3T5Q, 3T5N, 4FVU and 4GV9 [20-24]. The NP for the RNA synthesis and immune suppression (3MWP, 3MWT, 3MX2, 3MX5) [20], the arenavirus NP for the genomic ribonucloe protein complexes, (3T5Q and 3T5N) [21] which are critical for transcription and replication of the viral genome, involving in RNA-binding domain of Lassa virus NP in complex with ssRNa. 4FVU [22] involves indigestion of NP exonuclease activity, which causes suppression of innate immune signaling in the infected cell, and 4GV9,3'-5' exoribonuclease [23] suppresses type 1 interferon (IFN) production by degrading the immune stimulatory RNAs.

The protein receptors were downloaded from the Protein Data Bank (PDB), a depository data bank that contains 3D structural information of large biological molecules such as proteins and nucleic acids (https://www.rcsb.org/structure). Also, the SDS format of the ligands was gotten from the PubChem database (https://pubchem.ncbi.nlm.nih.gov) and then taken to cactus online smiles translator (https://cactus.nci.nih.gov) for ligand download.

IN-SILICO METHODS:

Molecular Docking Procedures: The equilibrium conformers were searched for downloaded ligands with Austin Model 1 (AM1) of the semi-empirical AM1 method. The lowest energy conformer of each ligand was used as starting structure for optimization with Density Functional Theory (DFT) method of Becke's three-parameter hybrid functional with correlation of Lee, Yang and Parr (B3LYP) [24, 25] with 6-31G** basis set. The minima equilibrium optimization was verified by frequency calculations characterized by positive harmonic frequencies [26, 27] as implemented in Spartan 14 [28]. These optimized structures of the ligands were now used for molecular Dockingsimulations. Docking of the proteins with the ligands or inhibitors was carried out using Discovery studio, Autodock Tool 1.5.6. On the Autodock tool, AutoDock Vina 1.1.2 and Edupymol version 1.7.4.4. Discovery studio was used to clean up and repair the receptor, while Edupymol was used as a visualizer. Autodock Tool was used to set the grid box around the binding site

of the proteins as observed in the crystal structures, polar hydrogen atoms were first added to the proteins followed by Gasteiger charges calculation before setting the grid box. The protein files were saved as pdbqt file prior to docking simulation with AutoDock Vinato to calculate binding affinity and Interactions between the ligand and proteins were visualized using discovery studio 2019 [29-39]. However, 3DLigandSite -Ligand binding site prediction Server (https://www.wass-michaelislab.org/3dlig/) was used to identify the active gorge of the proteins based on ligand-binding sites predictions using similar structures [40].

Pharmacokinetics Profile: The smiles structures of drugs/ ligands downloaded from the PubChem database were used for the physicochemical and ADMET profiles of the ligands to assess the qualitative pharmacokinetics properties *viz;* absorption, distribution, metabolism, excretion, and toxicity by using ADMET Predictor 9.5 installation (www.simulations-plus.com).

RESULTS AND DISCUSSION:

Docking Conformation and Binding Affinity:

Docking with 3 MWP: Several conformations were achieved from the docking simulation of the studied compounds. The superlative conformation (conformation with lowest binding free energy) is presumed to be the conformation with binding energy in relation to the inhibitory constant (Ki).

The predicted binding energies for all the studied drugs (Bergamottin, Casticin, Lacidipine, Phenothrin, Remdesvir and Ribavirin) with 3 MWP receptor showed that Remdesvir has the binding affinity of -9.1 kcal/mol; Phenothrin -8.6 kcal/mol, Casticin -8.3 kcal/mol, Bergamottin -7.2 kcal/mol, Ribavirin -6.5 kcal/mol and Lacidipine -6.3 kcal/mol.

The inhibitory constant (Ki) of the drugs ranges from 0.21 – 23.96µM; Remdesvir 0.21 µM, Phenothrin 0.49 µM, Casticin 0.82 µM, Bergamottin 5.24 µM, Ribavirin 17.10 µM and Lacidipine 23.96 µM; the higher the binding affinity, the lower the inhibition constant and vice versa [41] as shown in **Table 1**. The H-bond distances between amino acid residues in the binding purse and drug range from 1.8 to 3.5Å, and other forms of interactions between the ligand and the receptor are displayed in **Fig. 1**.

TABLE 1: BINDING AFFINITY AND NON-BONDING INTERACTIONS OF 3MWP RECEPTOR WITH THE LIGANDS

Ligands	Binding Affinity ΔG (kcal/moll)	Inhibition constant K1 (µM)	3mwp receptor showing H-bond with ligands	H-bond distance (Å)	Non-bonding interactions
Bergamottin	-7.2	5.24	GLY'249, TYR'209	3.4, 2.1	SER'9, ARG'300, SER'308, ASN'305, GLU'299, LYS'253, THR'13, PRO'302, TYR'213, PHE'10
Casticin	-8.3	0.82	SER'9, TYR'209 GLU'266	2.3, 2.3,2.7 3.2	PRO'302, GLY'249, ALA'250, SER'247, THR'178, GLY'177, SER'238, LYS'253, LYS'309, ASN'305, TYR'319, TYR'213, THR'13, PHE'10
Lacidipine	-6.3	23.96	TRP'331, GLU'107 GLN'442	3.3, 3.2, 2.7	THR'334, LEU'106, LYS'110, ARG'561, GLN'369, THR'366, SER'368, VAL'336
Phenothrin	-8.6	0.49	ARG'300	2.8	GLY'177, LYS'309, TYR'308, LEU'312, ARG'323, ASN'174, ARG'329, ASN'173, ALA'169, SER'121, ARG'118, LEU'120, PHE'176, LEU'172, GLU'117, SER'238
Remdesvir	-9.1	0.21	ALA'169, LYS'167, LEU'550, VAL'549 ARG'556, GLU'170 ALA'169, ARG'118 ARG'118, ASN'168	1.9, 3.2,3.4 2.7, 2.6, 2.2, 3.2, 3.5, 2.6, 1.8, 3.1	ILE'114, ASP'557, TRP'331, ARG'329, ASN'173, PRO'555, SER'121, ARG'551, ALA'122, ALA'552, TYR'410, LEU'505, TYR'502
Ribavirin	-6.5	17.10	SER'238, GLU'117 ARG'300, ARG'300 ASN'174, ASN'174	2,7, 3.1, 2.4, 2.2, 3.1, 3.2	PHE'176, GLY'177, GLN'175, ARG'323, LEU'312, LYS'309, TYR'308, ARG'329, LEU'239

Bergamottin showed hydrogen bond with GLY'249 and TYR'209; Casticin formed H bond with SER'9, TYR'209 and GLU'266; Lacidipine with TRP'331, GLU'107 and GLN'442; Phenothrin with ARG'300; Remdesvir with LYS'167, LEU'550, VAL'549, ARG'556, GLU'170, ALA'169, ARG'118, ARG'118 and ASN'168; Ribavirin with SER'238, GLU'117, ARG'300, ARG'300 and ASN'174.

The order of binding affinity in relation to the drug activeness against 3MWP are Remdesvir > Phenothrine> Casticin > Bergamottin > Ribavirin > Lacidipine; thus, the conformation of the ligand in the active gouge of the receptor (3MWP) indicated that Remdesvir, Phenothrine, Casticin, and Bergamottin are more active inhibitors against 3MWP.

Therefore, botanical drugs (Casticin and Bergamottin) could serve as inhibitors against 3MWP, although Remdesvir and Phenothrine could be more potent.

Bergamottin

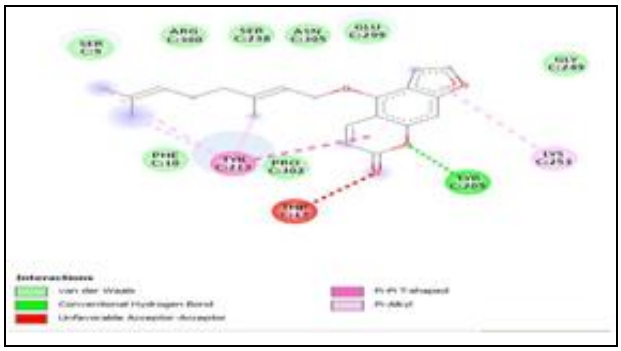

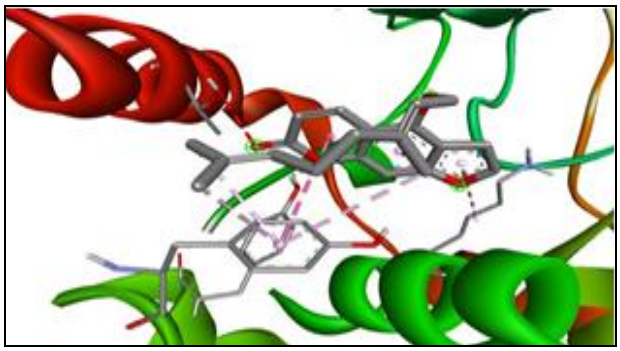

Casticin

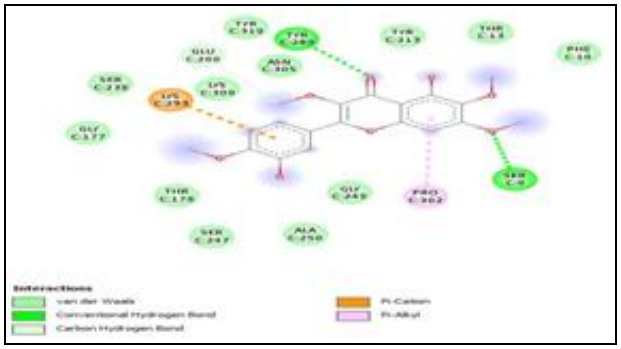

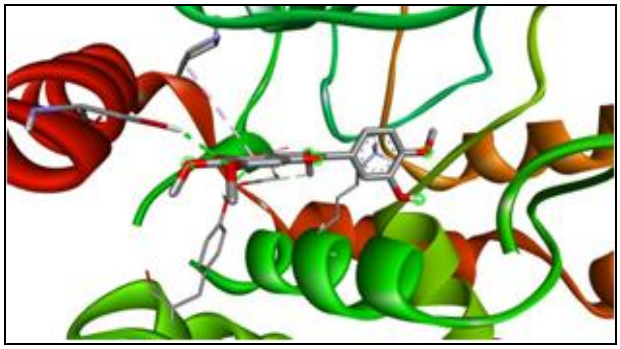

Lacidipine

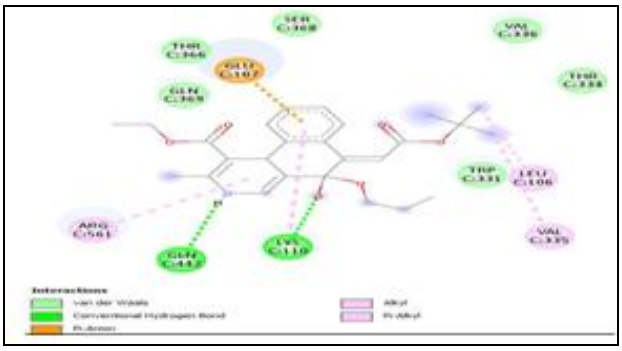

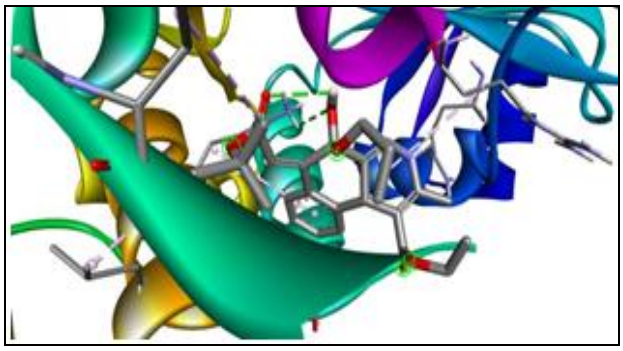

Phenothrine

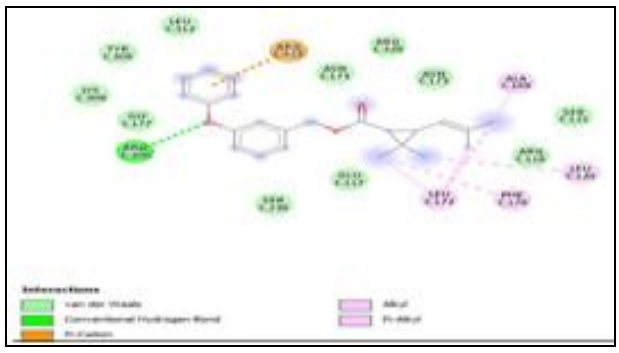

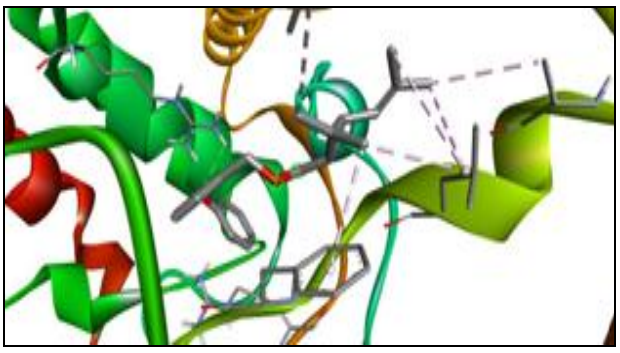

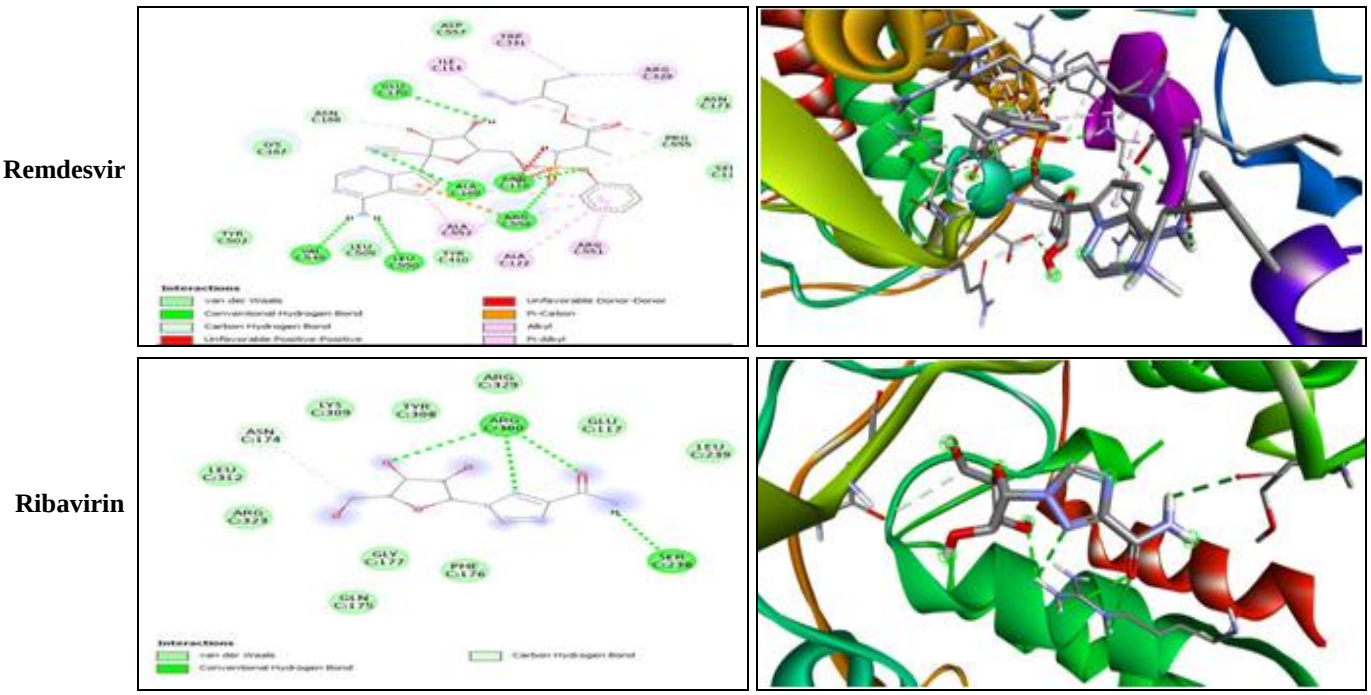

FIG. 1: THE BLIND DOCKED CONFORMATIONS OF INHIBITOR WITH 3MWP

Docking with 3MWT: Binding mode and scoring of these drugs **(**Bergamottin, Casticin, Lacidipine, Phenothrin, Remdesvir, and Ribavirin) with 3MWT receptor showed that all the drugs showed that Remdesvir also has the lowest binding affinity of -9.8 kcal/mol.

TABLE 2: BINDING AFFINITY AND NON-BONDING INTERACTIONS OF 3MWT RECEPTOR WITH THE LIGANDS

Ligands	Binding Affinity ΔG (kcal/moll)	Inhibition constant Ki (µM)	3mwt receptor showing H bond with ligands	H-bond distance (Å)	Electrostatic / Hydrophobic interactions
Bergamottin	-5.1	181.80	ARG'59, ASN'240	2.5, 2.7	SER'237, ASN'245, ARG'55, MET'54, ASP'233, ILE'241, LEU'239, GLY'145
Casticin	-6.9	8.70	ARG'492, ARG'492, ASP'533, GLU'391 GLU'391, ILE'390 GLN'425, ASP'426	1.9, 2.7, 3.4 3.1, 2.9,3.4 3.0, 3.0, 3.2	GLN'422, ARG'393, SER'430, GLY'392, ASP'389, PHE'537, LYS'488, HIS'528, TYR'429
Lacidipine	-7.4	3.74	GLY'249, TYR'213 GLU'219	3.3, 2.3, 3.0	PHE'10, SER'9, GLU'299, ARG'300, SER'238, THR'178, LYS'253, TYR'319, GLU'266, PRO'302, ASN'305, VAL'252, TYR'209, THR'13
Phenothrin	-5.7	66.00			LEU'140, ALA'139 GLN'136, ARG'137 GLN'133, LYS'374 LEU'378, MET'371 ASP'375, ARG'115
Remdesvir	-9.8	0.07	ASN'240, SER'238 ASN'305, ASN'305 SER'238	2.3, 2.0, 2.4 3.5, 2.5	PHE'176, TRP'164, ILE'241, LEU'120, THR'116, GLY'177, ASN'174, TYR'308, LYS'253, GLU'266, TYR'213, THR'13 TYR'209, LEU'265, PRO'302, GLY'249, GLU'299, GLU'117 LYS'309, ARG'300, LEU'239
Ribavirin	-6.6	14.44	PHE'176, GLN'175 ASN'174, GLU'117 GLU'117, ARG'323	2.2, 2.6, 2.6 2.7,3.0, 3.1 2.3	ARG'300, TYR'308, LEU'312, LYS'309, GLY'177, ARG'329 ASN'173, LEU'172

The binding affinities predicted are -7.4 kcal/mol for Lacidipine, -6.9 kcal/mol for Casticin, -6.6 kcal/mol for Ribavirin, -5.7 kcal/mol for Phenothrin and Bergamottin with-5.1 kcal/mol **Table 2.** The inhibition constant (Ki) of the drugs ranges from 0.07 – 181.80µM with Remdesvir having 0.07 µM and Bergamottin 181.80 µM. The H bond and other hydrophobic interactions showed that Casticin formed H bond with ARG'492, ARG'492, ASP'533, GLU'391, GLU'391, ILE'390, GLN'425 and ASP'426; and hydrophobic interactions with GLN'422, ARG'393, SER'430, GLY'392, ASP'389, PHE'537, LYS'488, HIS'528 and TYR'429. Lacidipine formed H bond with GLY'249, TYR'213 and GLU'219; Ribavirin with PHE'176, GLN'175, ASN'174, GLU'117, GLU'117 and ARG'323; Remdesvir with ASN'240, SER'238, ASN'305, ASN'305 and SER'238; Bergamottin with ARG'59 and ASN'240. Phenothrin only showed hydrophobic interactions with LEU'140, ALA'139, GLN'136, ARG'137, GLN'133, LYS'374, LEU'378, MET'371, ASP'375 and ARG'115 **Table 2** and **Fig. 2**.

Bergamottin

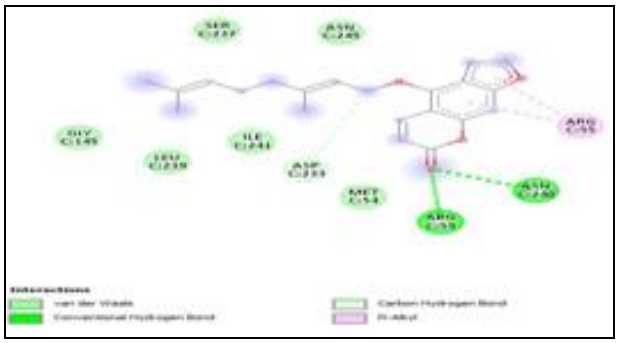

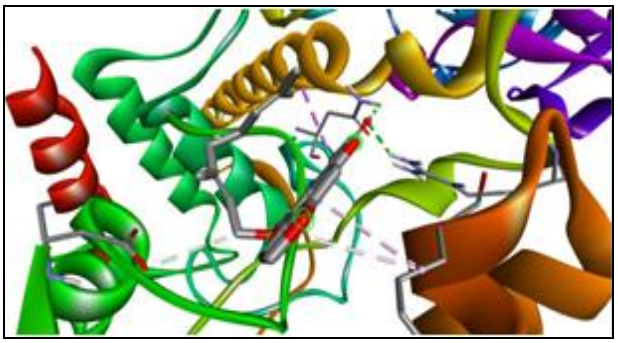

Casticin

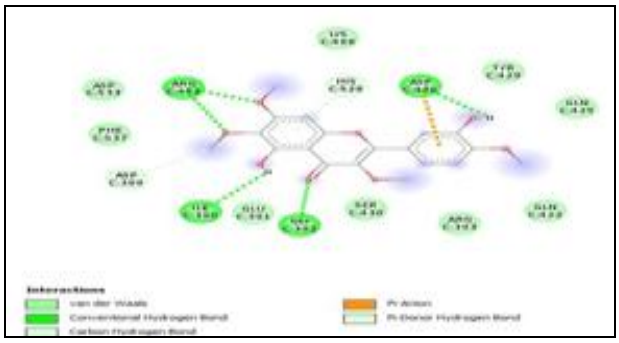

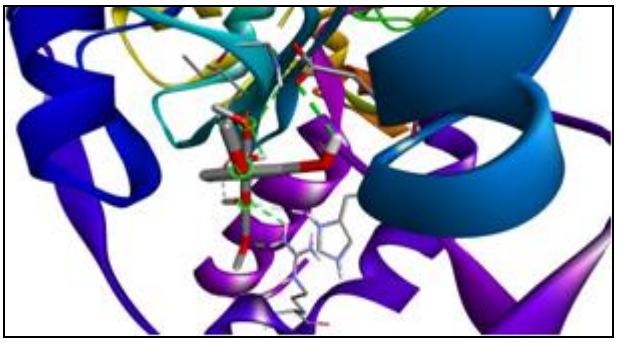

Lacidipine

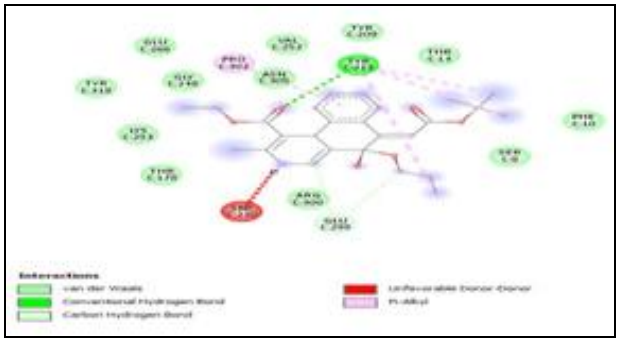

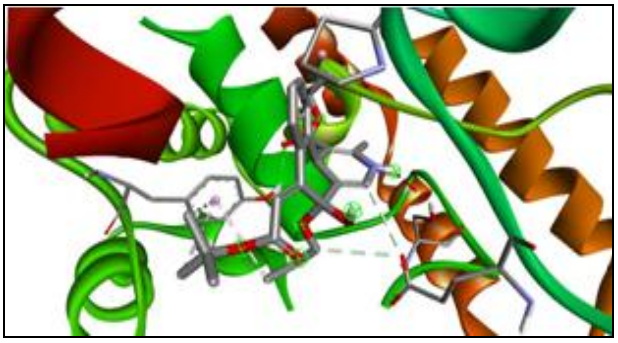

Phenothrine

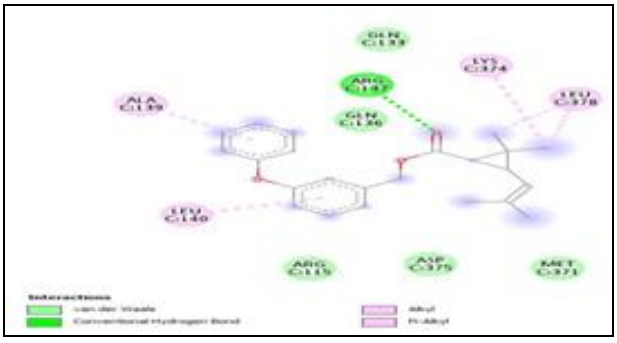

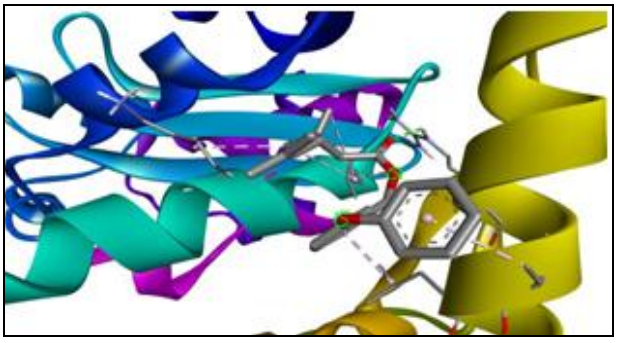

Remdesvir

Ribavirin

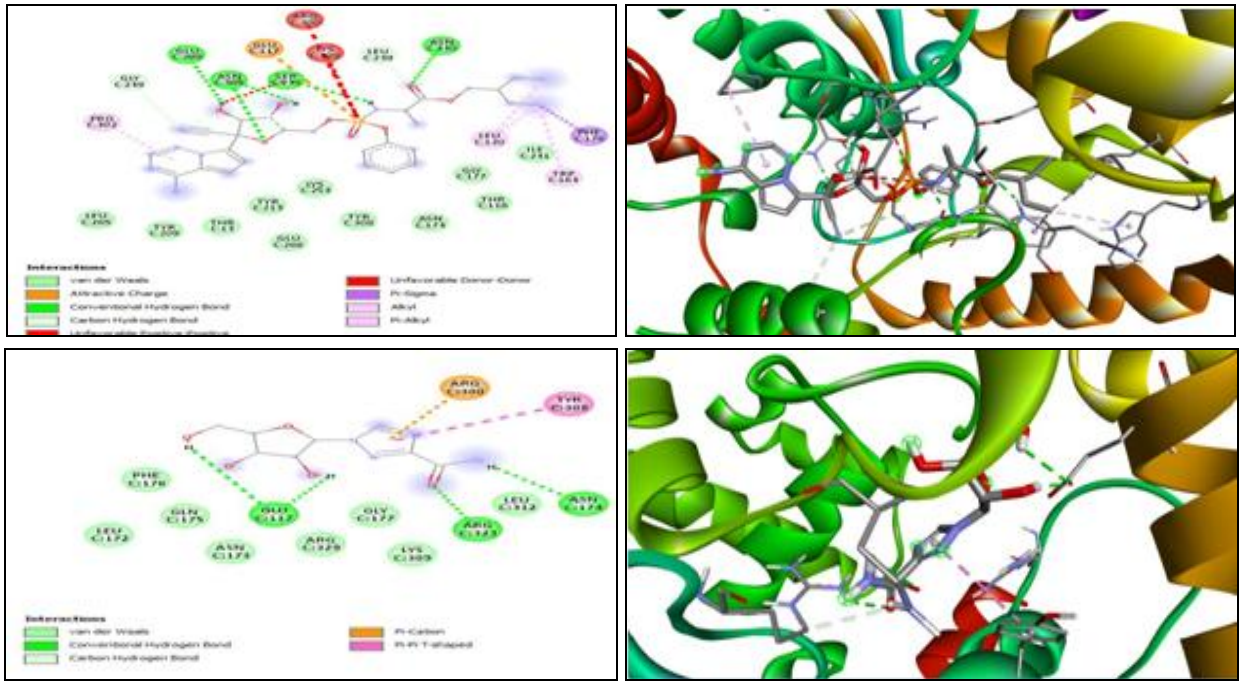

FIG. 2: THE BLIND DOCKED CONFORMATIONS OF INHIBITOR WITH 3MWT

The ordering of the affinity of these drugs 3MWT are Remdesvir >Lacidipine > Casticin >Ribavirin > Phenothrin > Bergamottin. This showed that Casticin could inhibit 3MWT, but Remdesvir and Lacidipine are more active inhibitors against 3MWT.

Docking with 3MX2: The superlative conformation of the drugs with 3MX2 showed that Bergamottin, Casticin, Lacidipine, Phenothrin, Remdesvir and Ribavirin have the lowest binding affinities of -6.0, -8.5, -7.8, -6.6, -10.5 and -6.2 kcal with inhibitory constant (Ki) 39.72, 0.58, 1.90, 14.44, 0.02 and 17.10 µM respectively **Table 3**. The ordering of the score values for these drugs with 3MX2 receptor is as: Remdesvir > Casticin > Lacidipine > Phenothrin > Bergamottin >.

TABLE 3: BINDING AFFINITY AND NON-BONDING INTERACTIONS OF 3MX2 WITH THE LIGANDS

Ligands	Binding Affinity ΔG (kcal/moll)	Inhibition constant Ki (µM)	3mx2 receptor showing H bond with ligands	H-bond distance (Å)	Electrostatic / Hydrophobic interactions involved
Bergamottin	-6.0	39.77	ARG'137	2.1	ASP'451, ARG'455, LEU'453, MET'377, PRO'454, GLN'133 GLN'136, GLN'132, LEU'378, LYS'374, ASP'375, ALA'452
Casticin	-8.5	0.58	THR'178, GLY'249 GLU'266, TYR'209	2.2, 3.0 3.2, 2.4, 2.7	LYS'253, LYS'309, TYR'209 THR'13, PHE'10, SER'9, TYR'213, PRO'302, SER'247 ALA'250, SER'238
Lacidipine	-7.8	1.90	ALA'552 LEU'550, ALA'169 ASN'168, GLU'170 GLU'170	2.4 3.3, 2.6, 3.0 2.1, 3.6	ALA'122, ALA'550, TYR'410, ARG'551, LEU'505, LYS'167 LEU'554, ARG'556, ARG'118, PRO'555
Phenothrin	-6.6	14.44			THR'13, PRO'302, ASN'305, TYR'209, ARG'300, THR'234 LEU'248, PRO'214, ASN'215, TYR'213, GLU'299
Remdesvir	-10.5	0.02	ASN'173, ARG'329 ARG'329, GLU'117 LEU'550, ALA'552 ARG'118	3.2, 2.5, 2.9 3.1, 3.4, 3.0, 2.2	LEU'172, ASP'557, GLU'332 ALA'169, PRO'555, ILE'115, GLU'170, LYS'167, VAL'549 ARG'551, ARG'556, LEU'554, ALA'122, SER'121, PHE'176

					TRP'164, LEU'120, LEU'172
Ribavirin	-6.2	17.10	TYR'319, TYR'209 ASN'305, TYR'209 GLU'266	2.4, 2.3, 2.2, 2.1, 2.5	THR'13, GLU'266, TYR'213, GLY'249, THR'178, LYS'253 LYS'309, SER'238, PRO'302, LEU'265, ARG'17

The 3MX2 residues in the binging gorge; ASP'451, ARG'455, LEU'453, MET'377, PRO'454, GLN'133, GLN'136, GLN'132, LEU'378, LYS'374, ASP'375 and ALA'452 formed hydrophobic interactions with Bergamottin, as well as H bond with ARG'137.

Lacidipine formed H bond with ALA'552, LEU'550, ALA'169, ASN'168, GLU'170 and GLU'170; Ribavirin displayed H bond interaction with TYR'319, TYR'209, ASN'305, TYR'209 and GLU'266; Remdesvir showed H bond with ASN'173, ARG'329, ARG'329, GLU'117, LEU'550, ALA'552 andARG'118; Casticin showed H bond with THR'178, GLY'249, GLU'266 and TYR'209.

Phenothrin only showed hydrophobic interactions with THR'13, PRO'302, ASN'305, TYR'209, ARG'300, THR'234, LEU'248, PRO'214, ASN'215 and TYR'213 **Table 3** and **Fig. 3**. This showed that Remdesvir, Casticin and Lacidipine are more active against 3MX2 than others drugs.

Bergamottin

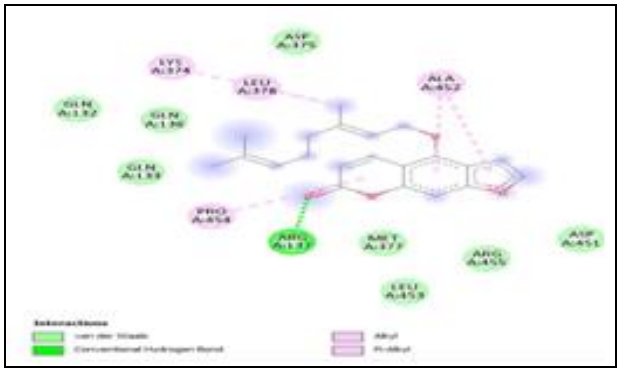

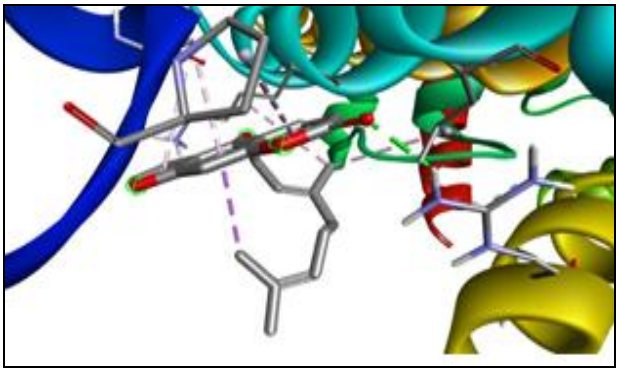

Casticin

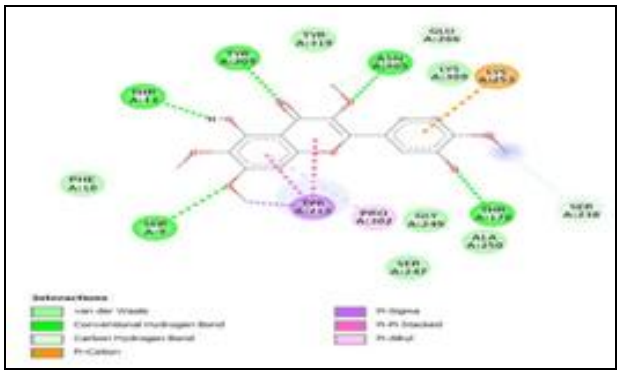

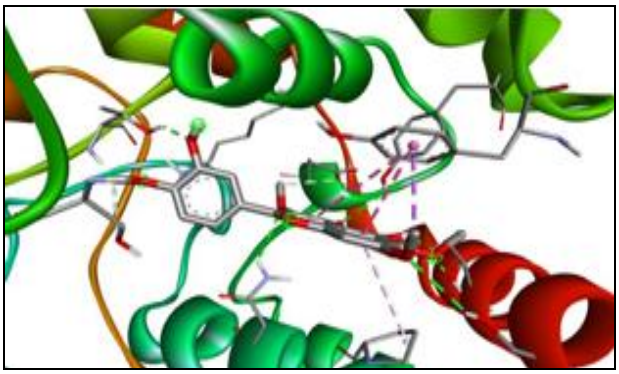

Lacidipine

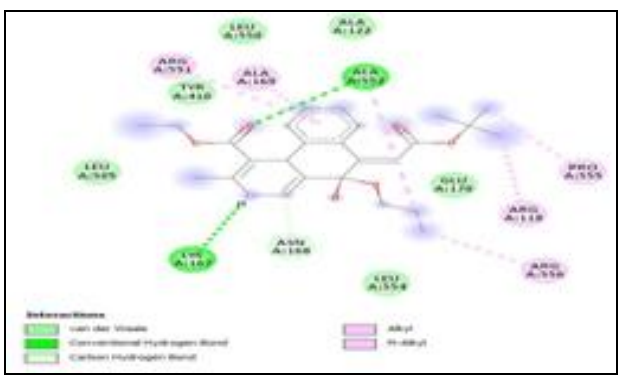

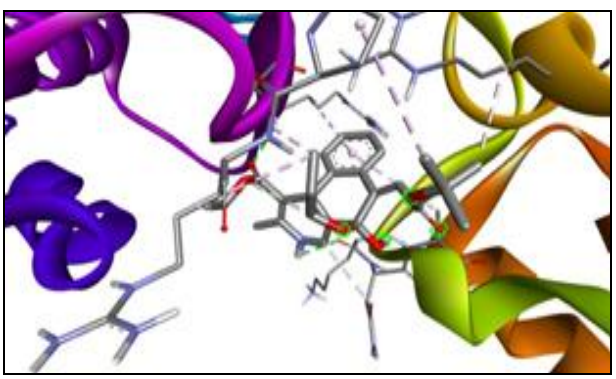

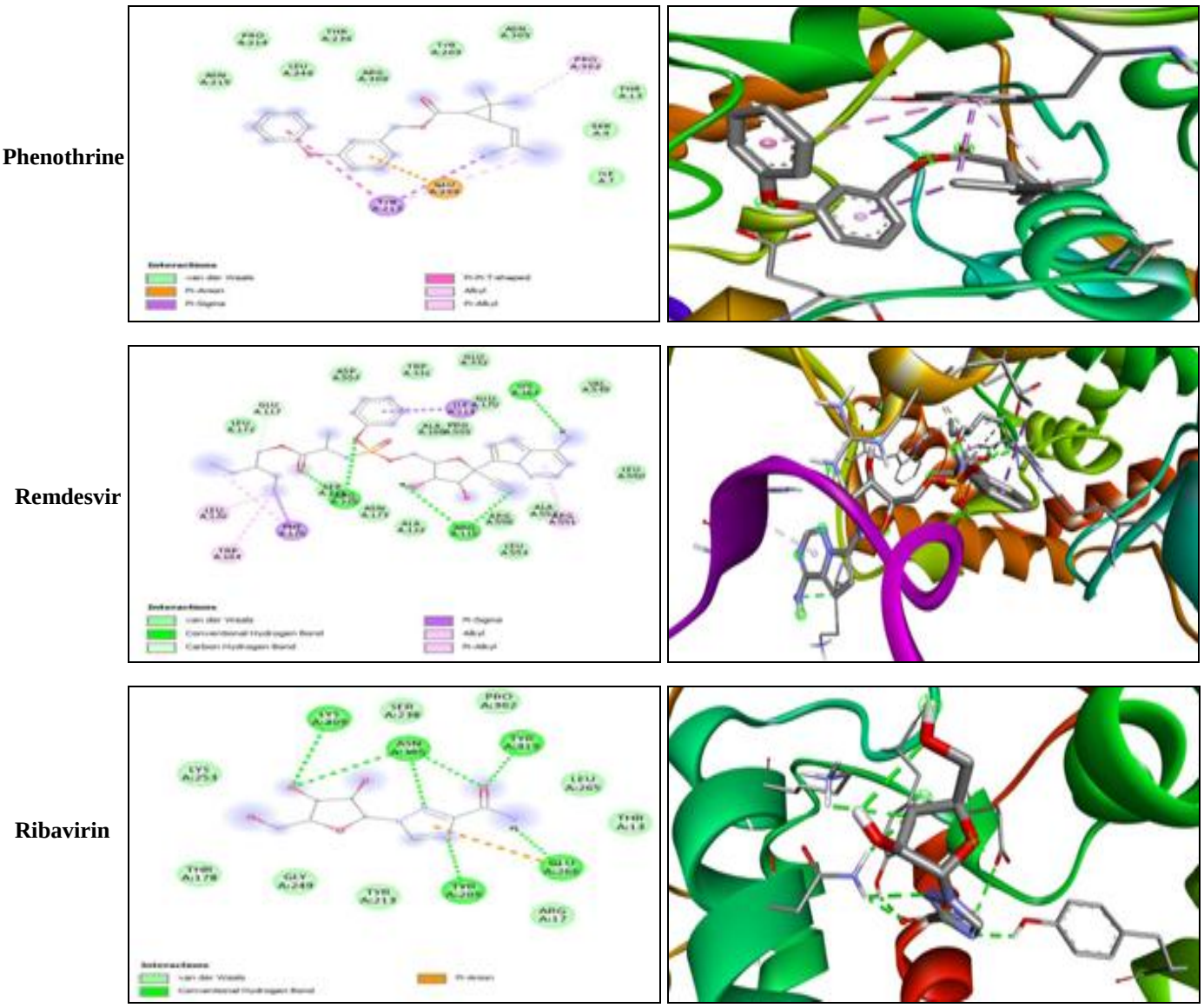

FIG. 3: THE BLIND DOCKED CONFORMATIONS OF INHIBITOR WITH 3MX2

Docking against 3MX5: Conformational interactions of the drugs with 3MX5 are displayed in **Table 4** and **Fig. 4**, the data from **Table 4** showed that the binding affinities predicted are -8.5 kcal/mol for Casticin, -8.4 kcal/mol for Lacidipine, -6.6 kcal/mol for Phenothrin, -6.5 kcal/mol for Ribavirin, - 10.1 kcal for Remdesvir and -8.1 kcal/mol for Bergamottin. The affinity ordered as Remdesvir > Casticin > Lacidipine > Bergamottin > Phenothrin > Ribavirin. Thus, it seemed that Remdesvir and Casticin are most active against 3MX5. The H bond and hydrophobic interactions of 3MX5 receptor with the drugs are shown in **Fig. 4**. Remdesvir formed H bond with ASN'305, GLU'117, LYS'309, ARG'323, PHE'176, THR'178, LYS'253 andLYS'309; Bergamottin displayed H bond interaction with GLY'298 and SER'238; Ribavirin formed H bond with ARG'329, GLU'117, ARG'323, ASN'240, PHE'176, GLY'117, PHE'176 and ILE'241; Casticin showed H bond with TRP'164 and hydrophobic interactions with LEU'172, SER'121, PHE'176, LEU'120, GLY'177, ARG'300, ARG'323, LYS'253, THR'178, ASN'305, LYS'309, SER'238, LEU'239, THR'116, ILE'241, GLU'117, MET'54, ASN'240 and ARG'59. Also, Lacidipine has H bond pose with ARG'300 and GLU'299, but hydrophobic interactions with LEU'248, SER'237, TYR'213, GLY'249, SER'9, PHE'10, THR'13, LEU'265, TYR'209, LYS'253, GLU'266, TYR'319, ASN'305, ASN'301, PRO'302 and SER'238; whereas Phenothrin displayed H bond with GLU'266 and hydrophobic interactions withARG'300, ASN'301, SER'238, GLY'249, LYS'253, LYS'309, TYR'319, LEU'265, ASN'305, TYR'209, THR'13, TYR'213, PRO'302, PHE'10 and SER'9.

TABLE 4: BINDING AFFINITY AND NON-BONDING INTERACTIONS OF 3MX5 WITH THE LIGANDS

Ligands	Binding Affinity ΔG (kcal/moll)	Inhibition constant Ki (µM)	3mx5 receptor showing H bond with ligands	H-bond distance (Å)	Electrostatic / Hydrophobic interactions
Bergamottin	-8.1	1.15	GLY'298, SER'238	3.0, 3.2	GLY'299,THR'116, LEU'239, ASN'174, ARG'323, ASN'240, ILE'241, LEU'120, LEU'172, GLY'177, GLU'117, PHE'176, LYS'309, THR'178, SER'238, ARG'300
Casticin	-8.5	0.58	TRP'164	2.3	LEU'172, SER'121, PHE'176, LEU'120, GLY'177, ARG'300, ARG'323, LYS'253, THR'178, ASN'305, LYS'309, SER'238, LEU'239, THR'116, ILE'241, GLU'117, MET'54, ASN'240 ARG'59
Lacidipine	-8.4	0.69	ARG'300, GLU'299	3.2, 3.5	LEU'248, SER'237, TYR'213, GLY'249, SER'9, PHE'10, THR'13, LEU'265, TYR'209, LYS'253, GLU'266, TYR'319 ASN'305, ASN'301, PRO'302, SER'238
Phenothrin	-6.6	14.44	GLU'266	3.3	ARG'300, ASN'301, SER'238, GLY'249, LYS'253, LYS'309, TYR'319, LEU'265, ASN'305, TYR'209, THR'13, TYR'213 PRO'302, PHE'10, SER'9
Remdesvir	-10.1	0.04	ASN'305, GLU'117 LYS'309, ARG'323 PHE'176, THR'178 LYS'253, LYS'309	2.7, 3.2, 2.5, 2.4, 2.9, 2.4,2.8, 2.2, 2.3	GLY'177, ASN'174, ARG'329, ASN'173, ASN'240, SER'121 LEU'120, LEU'172, LEU'239, GLN'175, THR'116, ARG'300 SER'238, GLU'299
Ribavirin	-6.5	17.05	ARG'329, GLU'117 ARG'323, ASN'240 PHE'176, GLY'117 PHE'176, ILE'241	2.6, 3.0, 2.3, 2.3 2.3, 2.8, 3.5, 2.6, 3.5	LEU'120, LEU'239, SER'238, ARG'300, GLY'309, GLY'177, GLN'175, TYR'308, ASN'174

Bergamottin

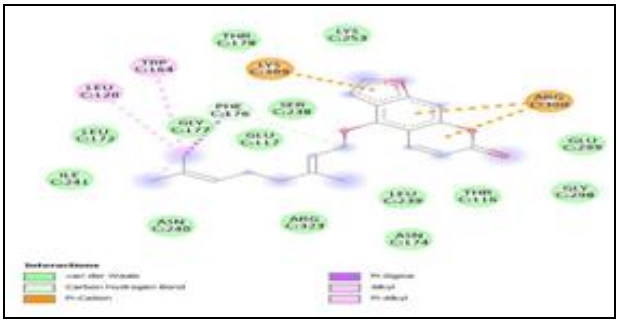

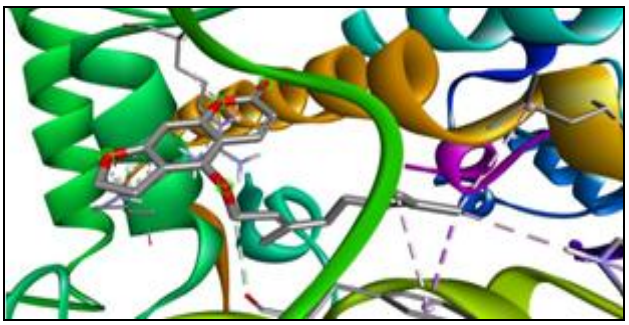

Casticin

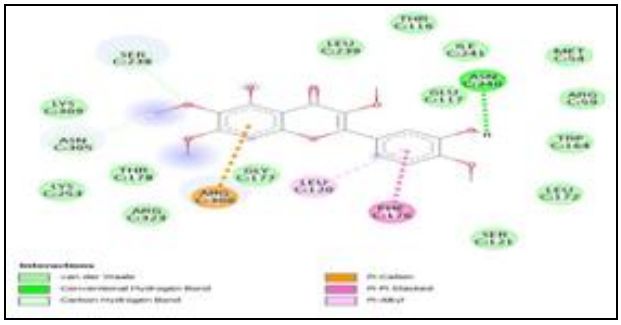

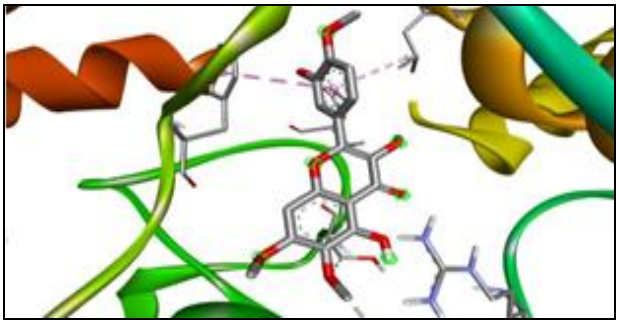

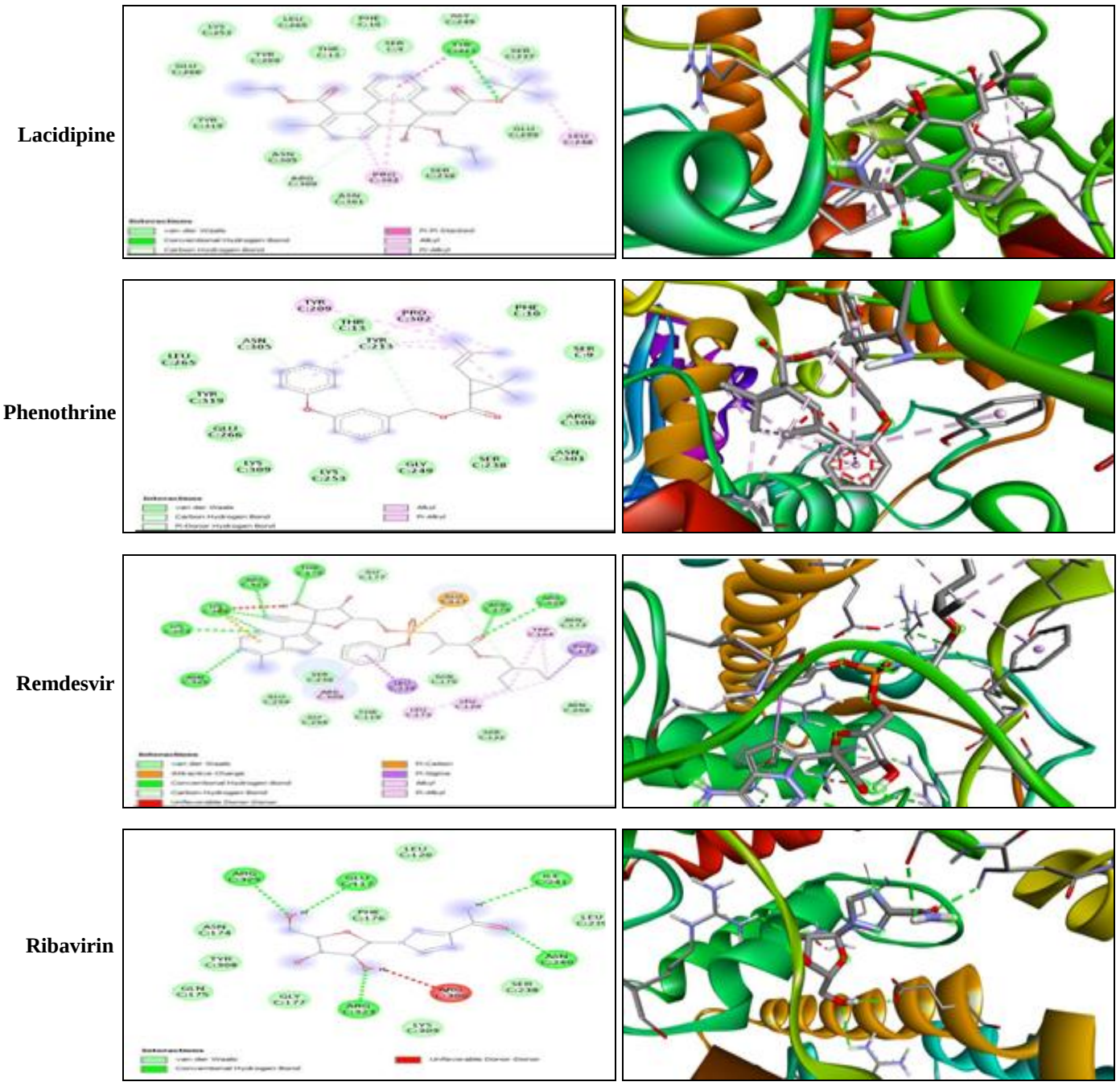

FIG. 4: THE BLIND DOCKED CONFORMATIONS OF INHIBITOR WITH 3MX5

Docking with 3T5N: Docking results of theseselected drugs with 3T5N are presented in **Table 5** and **Fig. 5.** The binding energies of the Bergamottin, Casticin, Lacidipine, Phenothrin, Remdesvir and Ribavirin are -8.2, -7.5, -7.1, -6.9, -8.7 and -6.2 kcal/mol with corresponding inhibitory constant (Ki) of 0.97, 6.21, 8.70, 0.42 and 28.37 µM respectively. This showed that Remdesvir and Bergamottin were presented with lowest binding affinity (*i.e* higher activity, 0.42 and 0.97 µM respectively); Lacidipine and have similar scoring affinity with 3T5N receptor. The binding affinity is ordered as Remdesvir > Bergamottin > Casticin > Lacidipine > Phenothrin > Ribavirin. Remdesvir formed H bond with ARG'300, ASN'240, ARG'329, ASN'174, GLY'177 and ARG'323; it also interacted hydrophobically withTYR'308, LYS'112,LEU'109, LYS'309, LYUS'253, THR'178, PHE'176, GLN'175, TRP'164, LEU'172, SER'172 and LEU'312. Bergamottin formed H-bond with ARG'323, LYS'309, ASN'174, ARG'329 and LEU'172; and hydrophobic interactions with PRO'297, LYS'112, LEU'109, TRP'331, SER'178, GLN'175, GLU'304, TYR'306, ARG'300, GLY'177

and LYS'258. Casticin is H bonded to GLY'309, LYS'253, ARG'323, ASN'174, LEU'172, PHE'176 and GLN'175; Lacidipine was H bonded to ARG'300, SER'9 and GLY'249; Ribavirin is H bonded to LYS'309, ARG'323, THR'178, LYS'253, PHE'176, GLN'175, ASN'174, ASN'174 and TYR'308, while Phenothrinis H bonded to GLU'266 **Fig. 5**. Therefore, Remdesvir and Bergamottin appeared as the most active against 3T5Q.

TABLE 5: BINDING AFFINITY AND NON-BONDING INTERACTIONS OF 3T5N WITH THE LIGANDS

Ligands	Binding Affinity ΔG (kcal/moll)	Inhibition constant Ki (μM)	3t5n Receptor showing H bond with ligands	H-bond distance (Å)	Electrostatic / Hydrophobic interactions involved
Bergamottin	-8.2	0.97	ARG'323, LYS'309, ASN'174, ARG'329 LEU'172	2.2, 2.6, 2.4, 2.5 3.3	PRO'297, LYS'112, LEU'109, TRP'331, SER'178, GLN'175 GLU'304, TYR'306, ARG'300, GLY'177, LYS'258
Casticin	-7.5	3.16	GLY'309, LYS'253 ARG'323, ASN'174 LEU'172, PHE'176 GLN'175	2.3, 2.2, 2.5, 2.6, 2.7, 2.1, 2.4 3.1, 2.2, 2.4	GLY'177, THR'178, ALA'250, SER'247, GLY'249, SER'173 ARG'329, ASN'174, TYR'308, ARG'300, ASN'214, LEU'239
Lacidipine	-7.1	6.21	ARG'300, SER'9 GLY'249	2.6,2.8, 2.1, 3.4	VAL'252, LYS'253, GLU'266, LEU'265, THY'13, ASN'305, TYR'209, TYR'319, PRO'302, TYR'213, LYS'309, ASN'301
Phenothrin	-6.9	8.70	GLU'266	3.4	ASN'301, PRO'302, ARG'300, ASN'305, THR'178, LYS'309, LYS'253, THR'319, GLY'249, VAL'252, TYR'319, TYR'209 TYR'213, SER'9
Remdesvir	-8.7	0.42	ARG'300, ASN'240, ARG'329, ASN'174 GLY'177, ARG'323	1.9, 2.5, 1.9,2.4 2.2, 2.7, 2.7	TYR'308, LYS'112, LEU'109, LYS'309, LYUS'253, THR'178, PHE'176, GLN'175 TRP'164, LEU'172, SER'172, LEU'312
Ribavirin	-6.2	28.37	LYS'309, ARG'323 THR'178, LYS'253 PHE'176, GLN'175 ASN'174, ASN'174 TYR'308	2.7, 2.7, 2.1, 2.5 2.1, 2.8, 2.4, 2.6 3.0, 3.4, 2.4	GLY'328, LEU'312, ARG'329, SER'173, LEU'172, ARG'300, GLY'177

Bergamottin

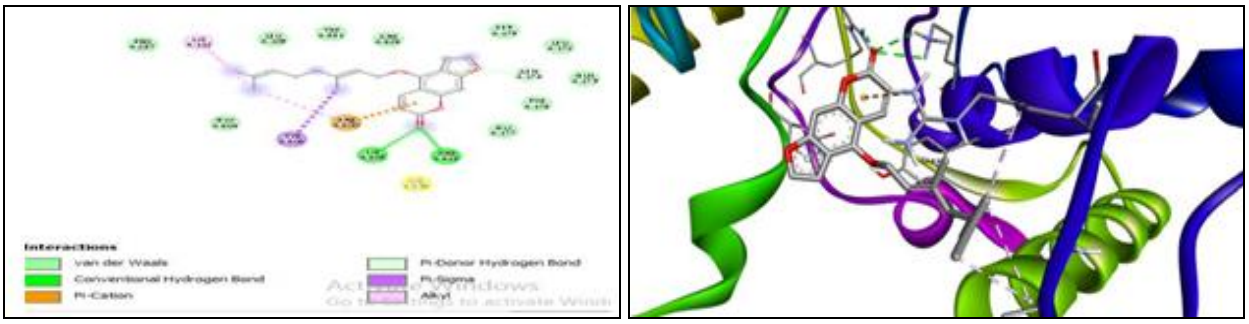

Casticin

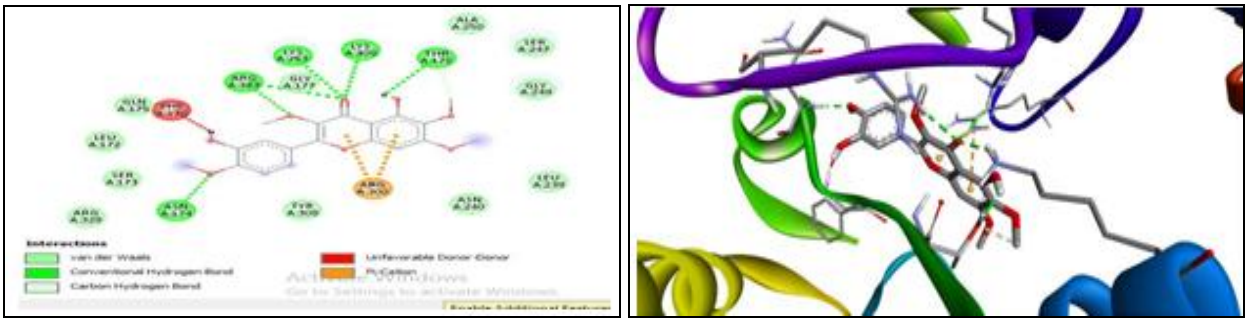

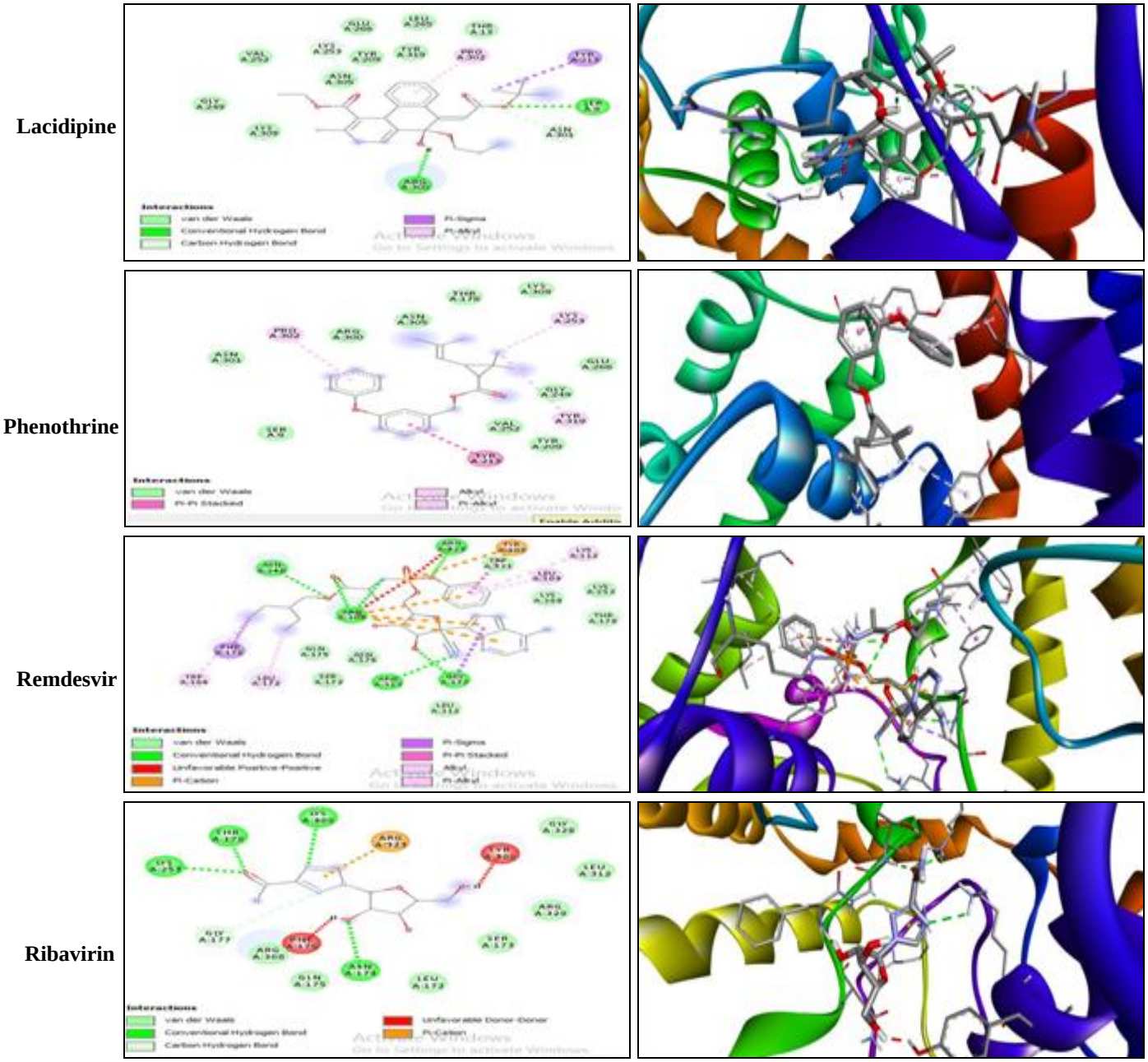

FIG. 5: THE BLIND DOCKED CONFORMATIONS OF INHIBITOR WITH 3T5N

Docking with 3T5Q: Docking of these drugs with **3T5Q** revealed that Bergamottin, Casticin, Lacidipine, Phenothrin, Remdesvir and Ribavirin have binding affinity values of -7.1, -7.4, -7.4,-7.0, -9.2 and -5.8 kcal/mol, respectively; it is obvious that Remdesvir has the highest score with inhibitory constant (Ki) of 0.18 µM **Table 6**. Casticin and Lacidipine presented the affinity value, while that of Bergamottin and Phenothrin are quite similar in values but higher than Ribavirin. Remdesvir is H bonded to SER'247, THR'178, ARG'300, ARG'300, ARG'300, LYS'253, THR'178, ARG'323, ARG'323, ASN '174, LEU'172, PHE'176 andGLN'175, and interacted hydrophobically with GLY'249, ALA'250, GLY'177, LYS'309, SER'173, ASN'240, TRP'164, LEU'239, ARG'329, THR'308, LEU'109 and SER'238. Casticin is H bonded to ARG'300, ARG'300 and ARG'323, and it formed hydrophobic interactions with LYS'309, GLY'177, ASN'174, SER'173, LEU'172, PHE'176, ALA'179, LEU'312, TYR'308, ARG'300, ARG'329, ASN'240 and TRP'164. Bergamottin formed H bond with PRO'302 and TYR'209; Phenothrin has H bond pose with GLY'249 and Ribavirin is H-bonded to ASP'233, MET'231, PHE'246, ARG'55, ASN'245 and GLN'51as shown in **Table 6** and **Fig. 6.**

TABLE 6: BINDING AFFINITY AND NON-BONDING INTERACTIONS OF 3T5Q WITH THE LIGANDS

Ligands	Binding Affinity ΔG (kcal/moll)	Inhibition constant K1 (μM)	3t5q receptor showing H bond with ligands	H-bond distance (Å)	Electrostatic / Hydrophobic interactions involved
Bergamottin	-7.1	6.21	PRO'302 TYR'209	3.3 2.1	LYS'309, LYS'253, ARG'300, TYR'213, TYR'319, SER'9, LEU'265, ILE'306, ASN'305, GLY'249
Casticin	-7.4	3.74	ARG'300, ARG'300 ARG'323	2.5, 2.5 2.6 2.5	LYS'309, GLY'177, ASN'174, SER'173, LEU'172, PHE'176, ALA'179, LEU'312, TYR'308, ARG'300, ARG'329, ASN'240 ,
Lacidipine	-7.4	3.74	TYR'209, PRO'214	1.9 3.4	LEU'265, ILE'306, THR'13, PRO'302, ASN'301, ARG'300, THR'213, SER'9, ASN'215, ASN'305 THR'319, GLU'266, GLY'249, VAL'252, LEU'248
Phenothrine	-7.0	7.35	GLY'249	3.0	LYS'253, GLU'266, LYS'309, TYR'319, ASN'305, LEU'265, THR'13, ASN'301, PRO'302, ARG'300, VAL'252, SER'9, TYR'209, TYR'213, PRO'214
Remdesvir	-9.2	0.18	SER'247, THR'178 ARG'300, ARG'300 ARG'300, LYS'253 THR'178, ARG'323 ARG'323, ASN '174, LEU'172, PHE'176, GLN'175	1.9, 2.8, 2.3, 2.3, 2.4, 2.3,2.5, 2.2, 2.2, 2.0, 2.2 3.0, 2.4, 2.7	GLY'249, ALA'250, GLY'177, LYS'309, SER'173, ASN'240, TRP'164, LEU'239, ARG'329, THR'308, LEU'109, SER'238
Ribavirin	-5.8	55.74	ASP'233, MET'231 PHE'246, ARG'55 ASN'245, GLN'51	1.8, 2.9, 3.0 2.3, 2.1, 3.3 2.8	SER'237, LYS'236, ARG'52, SER'48 ILE'232

Bergamottin

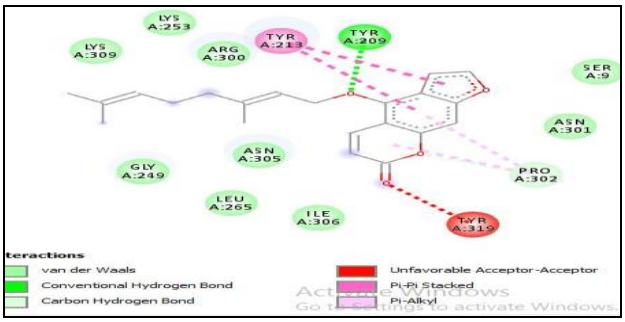

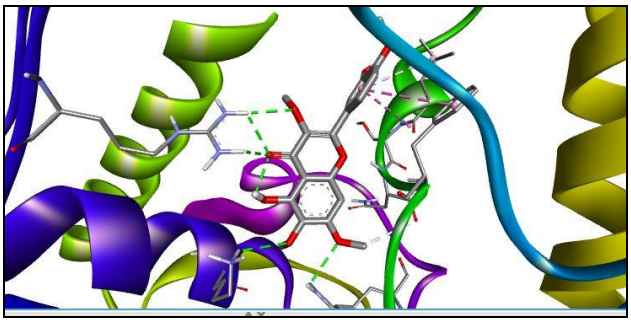

Casticin

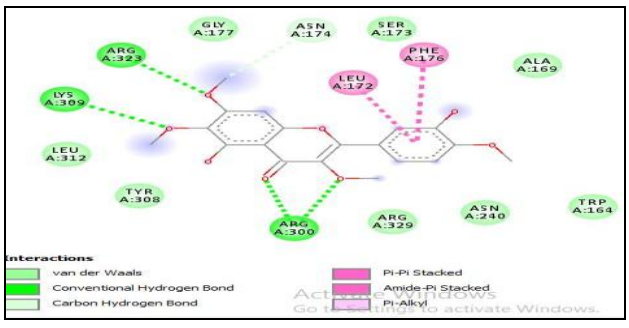

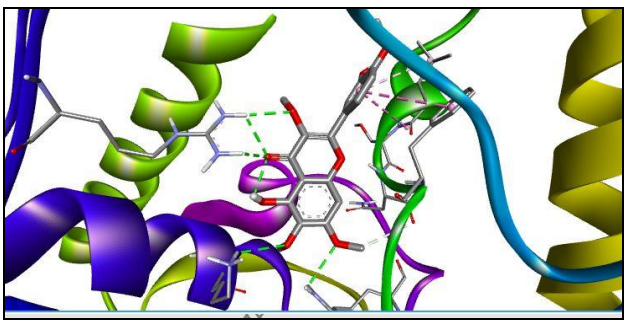

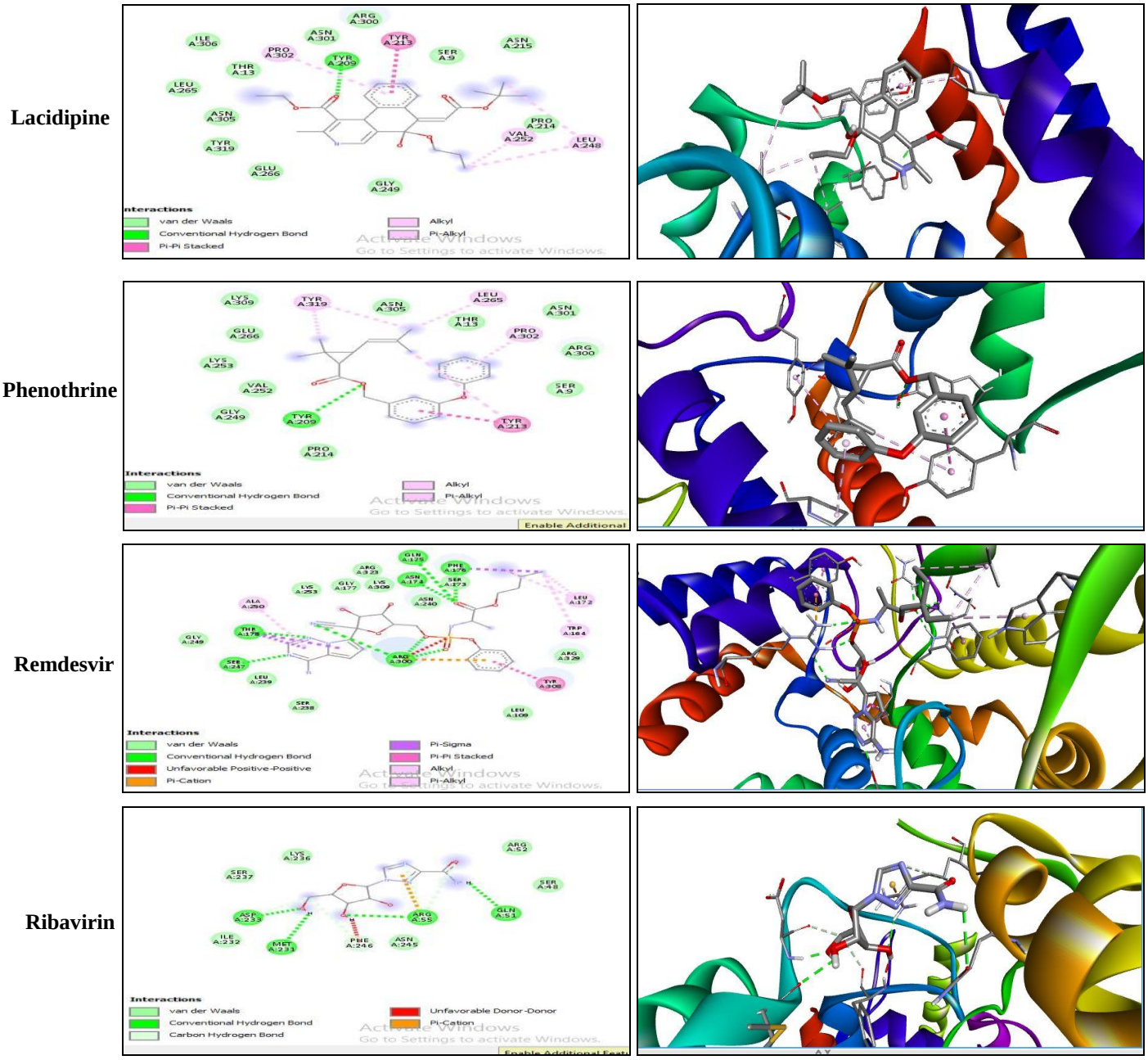

FIG. 6: THE BLIND DOCKED CONFORMATIONS OF INHIBITOR WITH 3T5Q

Docking against 4FVU: Docking mode analysis and binding affinity predicted for the drug-4FVU complex showed that the binding affinity of the most stable conformation of the drugs are -7.1, -6.9, -6.1, -5.2, -7.9 and -6.3 kcal/mol for Bergamottin, Casticin, Lacidipine, Phenothrine, Remdesvir and Ribavirin respectively; this showed that Remdesvir and Bergamottin are most active, affinity value of Casticin (-6.9 kcal) is similar to that of Bergamottin as shown in Table 7. Remdesvir formed H-bond with GLY'392, ASP'533, ARG'492, ARG'492, ARG'492, SER'491, ASP'389, GLN'462, ILE'390, ASP'466, GLY'463, ASP'426 and GLN'462, but interacted hydrophobically withGLU'515, ILE'525, LEU'486, SER'487, LYS'488, PHE'537, HIS'528, ARG'393, HIS'431, SER'430 and ALA'391. Bergamottin showed H-bond with HIS'412 and HIS'507, andhydrophobic interactions with ALA'440, ARG'556, ASP'437, PHE'560, VAL'559, TYR'410, PHE'414, LEU'505, TYS'506and MET'508. Casticin is H-bonded to ASP'389, ILE'390, GLY'392, ARG'492 and GLN'462; Lacidipine is H-bonded to ARG'492, ARG'492, HIS'528, ASP'426 and ARG'393; Ribavirin formed H-bond with ARG'492, ASP'533, ASP'389, HIS'528, ILE'390, GLY'392, ASP'466, ASP'426 and ARG'393, where as Phenothrine is H-bonded to TYR'410 **Fig. 7.**

TABLE 7: BINDING AFFINITY AND NON-BONDING INTERACTIONS OF 4FVU WITH THE LIGANDS

Ligands	Binding Affinity ΔG (kcal/moll)	Inhibition constant Ki (μM)	4fvu receptor showing H bond with ligands	H-bond distance (Å)	Electrostatic / Hydrophobic interactions involved
Bergamottin	-7.1	6.21	HIS'412, HIS'412 HIS'507	3.4, 2.3 2.1	ALA'440, ARG'556, ASP'437, PHE'560, VAL'559, TYR'410 PHE'414, LEU'505, TYS'506, MET'508
Casticin	-6.9	8.70	ASP'389, ILE'390 GLY'392, GLY'392 ARG'492, GLN'462	3.5, 2.9 2.1, 3.5 2.5, 2.3	GLY'463, PHE'537, GLN'462, ASP'533, HIS'528, ALA'391, SER'430, ASP'426, HIS'431,, ARG'393, ASP'466, LYS'488, SER'491, LEU'486
Lacidipine	-6.1	33.59	ARG'492, ARG'492 HIS'528, ASP'426, ARG'393	2.1, 2.7, 2.5, 3.4 2.5	ASP'466, ALA'391, ILE'390, HIS'431, GLY'392, SER'430, PRO'394, TYR'429, PHE'537, GLN'462, GLY'463, LYS'488
Phenothrine	-5.2	153.55	TYR'410	2.3	PHE'563, PHE'414, HIS'412, PHE'413, ALA'552, CYS'506, LEU'505, ARG'556, HIS'507, MET'508, VAL'559
Remdesvir	-7.9	1.61	GLY'392, ASP'533, ARG'492, ARG'492 ARG'492, SER'491 ASP'389, GLN'462, ILE'390, ASP'466, GLY'463, ASP'426, GLN'462	2.4, 3.1, 2.4, 2.6, 2.2, 2.2, 2.2, 3.0, 2.8, 3.1, 2.9,3.2 3.2, 2.5, 2.1	GLU'515, ILE'525, LEU'486, SER'487, LYS'488, PHE'537 HIS'528, ARG'393, HIS'431, SER'430, ALA'391
Ribavirin	-6.3	23.96	ARG'492, ARG'492, ASP'533, ASP'389 HIS' 528, ILE'390, GLY'392, GLY'392, ASP'466, ASP'426 ARG'393	2.7, 2.2, 2.9, 2.8, 2.6, 3.0 3.5, 3.6, 2.2 2.8, 2.7, 2.8	HIS'431, ALA'319, SER'430 PHE'537, GLN'462

Bergamottin

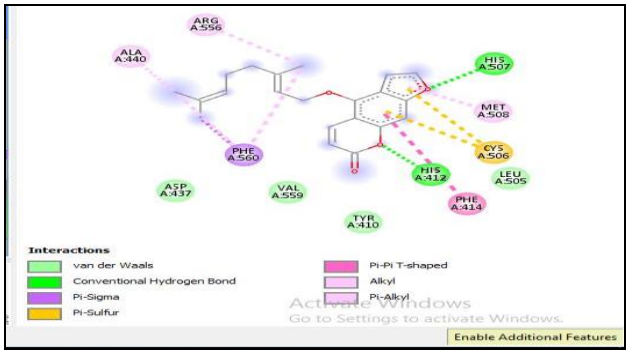

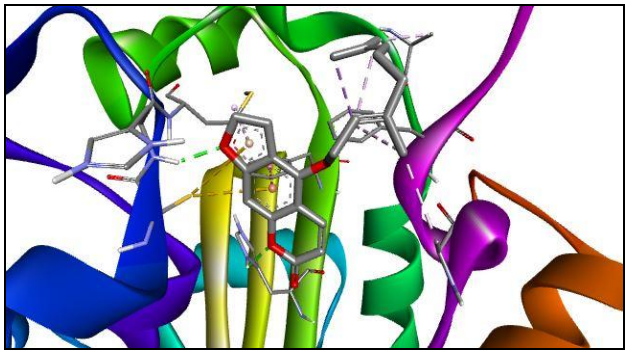

Casticin

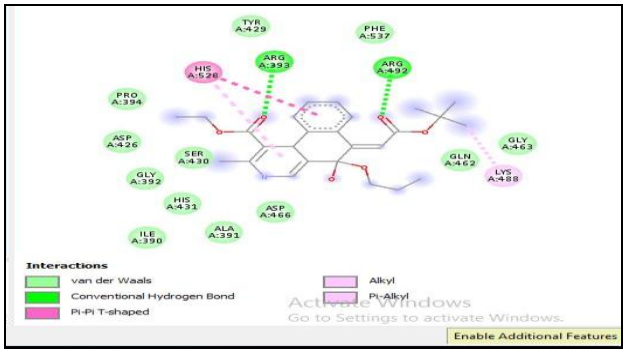

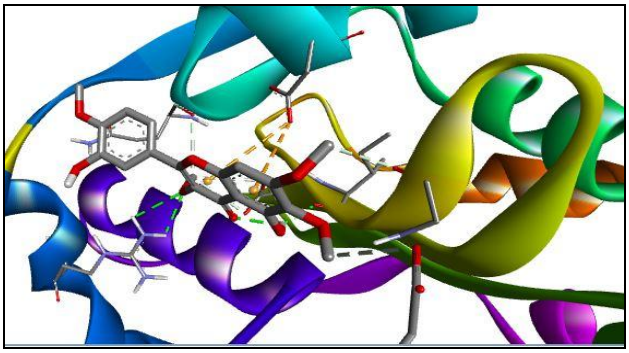

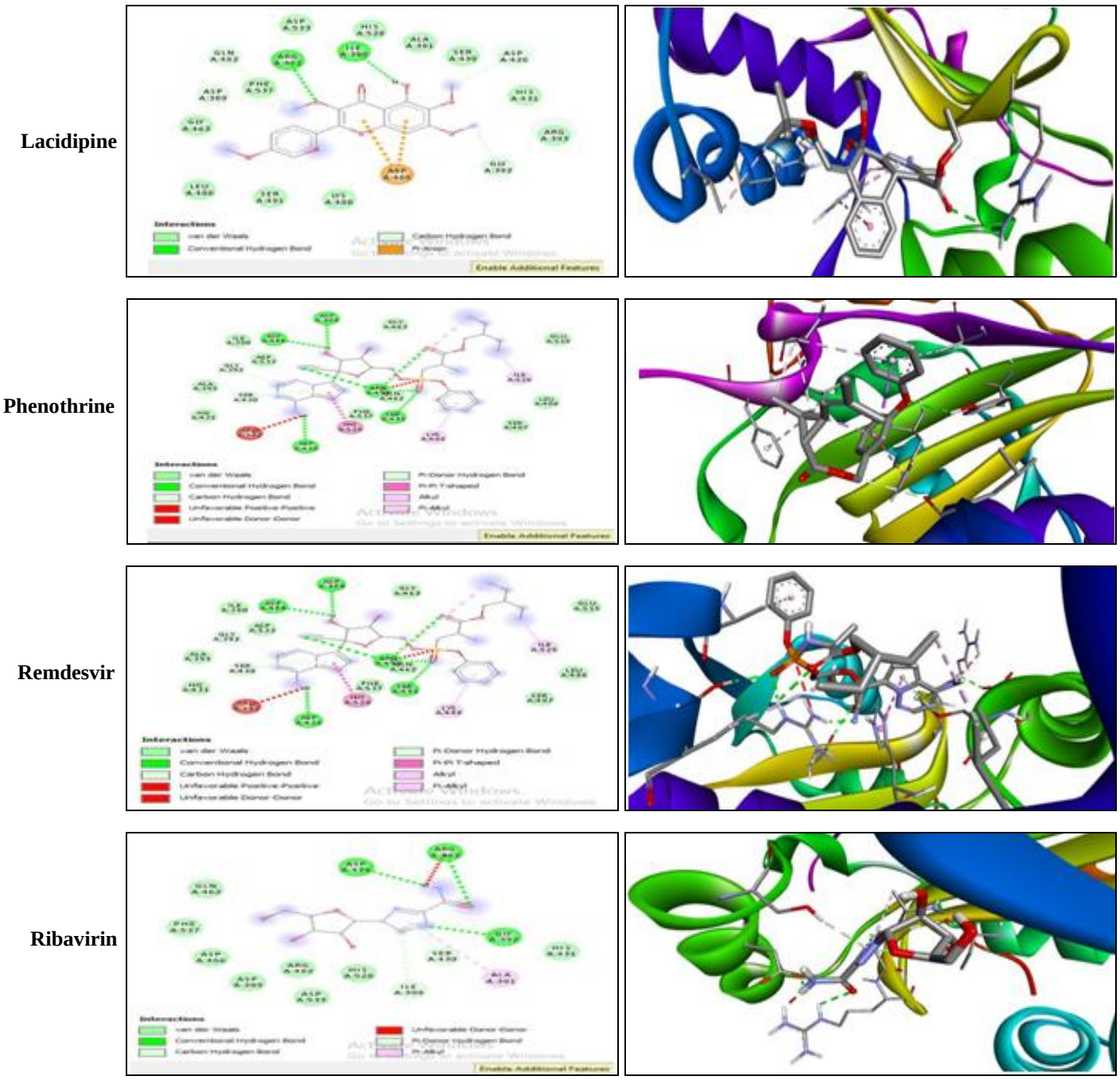

FIG. 7: THE BLIND DOCKED CONFORMATIONS OF INHIBITOR WITH 4FVU

Docking against 4GV9: The binding score energy results of the drugs toward 4GV9 protein showed that Bergamottin, Casticin, Lacidipine, Phenothrine, Remdesvir and Ribavirin have the binding score energy values of -6.7, -7.0, -6.5, -6.0, -7.7 and -6.2 kcal/mol, respectively as presented in **Table 8**. The binding affinity valves with 4GV9 for the drugs is ordered as Remdesvir >Casticin >Bergamottin >Lacidipine >Ribavirin > Phenothrine, this showed that Remdesvir and Casticin are active although the affinity values of Phenothrine and Ribavirin are similar.

Casticin is H-bonded to ARG'349, ARG'393, SER'430, ILE'390, GLU'391, ASP'533 and GLU'391, and having hydrophobic interactions with GLN'425, ASP'426, TYR'429, GLY'392, ASP'389, PHE'537, ARG'393, HIS'528, ARG'492 and LYS'488. Remdesvir formed H-bond with GLN'462, GLY'392, SER'430, GLY'392, GLU'391, ILE'390, ASP'533 and TYR'429, and hydrophobically with ASP'389, PRO'394, ARG'492, HIS'431, LYS'488, HIS'528, GLN'425, ARG'393, ASP'426, ASP'466, PHE'537 and GLY'463. Ribavirin is H-bonded to GLY'392,

ASP'426, ASP'466, GLU'391, GLN'462, ILE'390, ASP'533, ASP'389 and GLU'391; Lacidipine is H-bonded to HIS'528, ARG'492 and GLU'391; Bergamottin is H-bonded to ASP'389, but has hydrophobic interactions with SER'487, SER'491, SER'430, ASP'533, PHE'537, LEU'486, ILE'390, ARG'492, LYS'488, GLN'462, GLU'391, ASP'466, GLY'392, GLY'463, ASP'465 and HIS'528. However, Phenothrine only exhibited hydrophobic interactions with PHE'537, SER'491, GLN'462, ARG'492, ASP'533, ASP'389, ILE'390, HIS'528, GLU'391, GLY'392, ARG'393, ASP'466, PRO'394, LYS'488, GLY'463 and SER'430.

TABLE 8: BINDING AFFINITY AND NON-BONDING INTERACTIONS OF 4GV9WITH THE LIGANDS

Ligands	Binding Affinity ΔG (kcal/moll)	Inhibition constant Ki (μM)	4gv9 receptor showing H bond with ligands	H-bond distance (Å)	Electrostatic / Hydrophobic interactions involved
Bergamottin	-6.7	12.19	ASP'389	3.6	SER'487, SER'491, SER'430, ASP'533, PHE'537, LEU'486, ILE'390, ARG'492, LYS'488, GLN'462, GLU'391, ASP'466, GLY'392, GLY'463, ASP'465, HIS'528
Casticin	-7.0	7.35	ARG'349, ARG'393, SER'430, ILE'390 GLU'391, ASP'533, GLU'391	2.4, 2.4, 2.7 2.8, 3.1,3.3 3.3, 3.2	GLN'425, ASP'426, TYR'429, GLY'392, ASP'389, PHE'537, ARG'393, HIS'528, ARG'492, LYS'488
Lacidipine	-6.5	17.09	HIS'528, ARG'492 GLU'391	2.1, 2.1, 2 .7	ASP'426, SER'430, ARG'393, TYR'429, PRO'394, PHE'537, SER'491, SER'430, GLN'462, LYS'488, GLY'463, ASP'466, ASP'533, ASP'389, GLY'392, HIS'431
Phenothrine	-6.0	39.77			PHE'537, SER'491, GLN'462, ARG'492, ASP'533, ASP'389, ILE'390, HIS'528, GLU'391, GLY'392, ARG'393, ASP'466, PRO'394, LYS'488, GLY'463, SER'430,
Remdesvir	-7.7	2.25	GLN'462, GLY'392 SER'430, GLY'392 GLU'391, ILE'390 ASP'533, TYR'429	2.3, 2.3, 2.4 2.7, 2.7, 2.8, 3.2, 3.3	ASP'389, PRO'394, ARG'492, HIS'431, LYS'488, HIS'528, GLN'425,ARG'393, ASP'426, ASP'466, PHE'537, GLY'463
Ribavirin	-6.2	28.37	SER'430, GLY'392 ASP'426, ASP'466 GLU'391, GLN'462 ILE'390, ASP'533 ASP'389, GLU'391	2.1, 2.3, 2.5 2.8, 2.9, 3.0 3.1, 3.1, 3.2 3.5	HIS'528, ARG'492, ARG'393, HIS'431, GLY'463

2D **3D**

Bergamottin

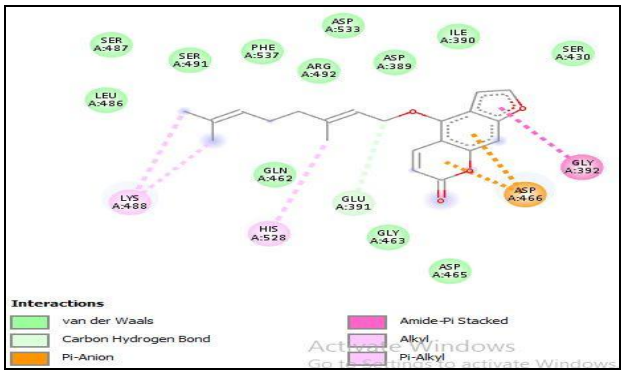

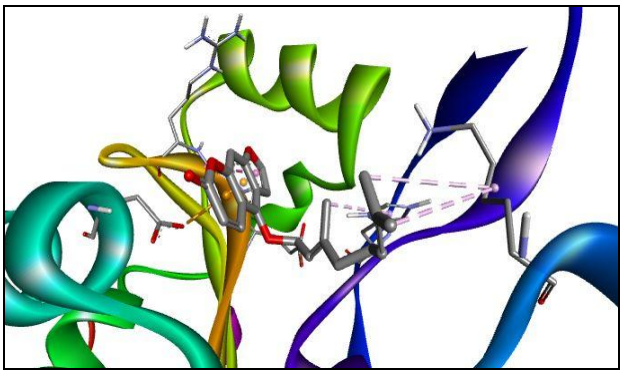

Casticin

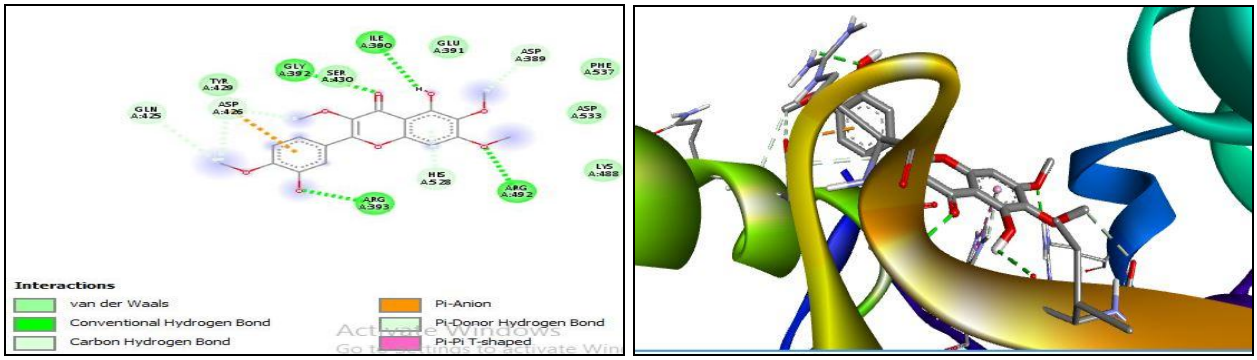

Lacidipine

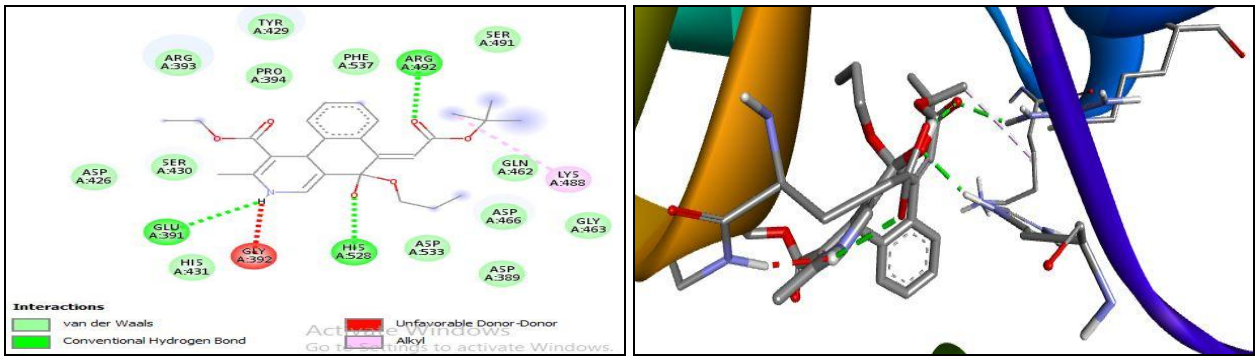

Phenothrine

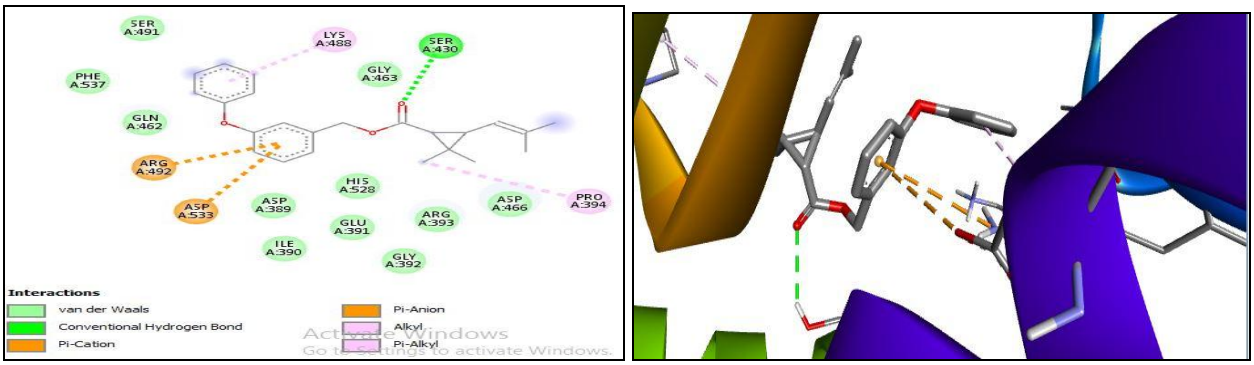

Remdesvir

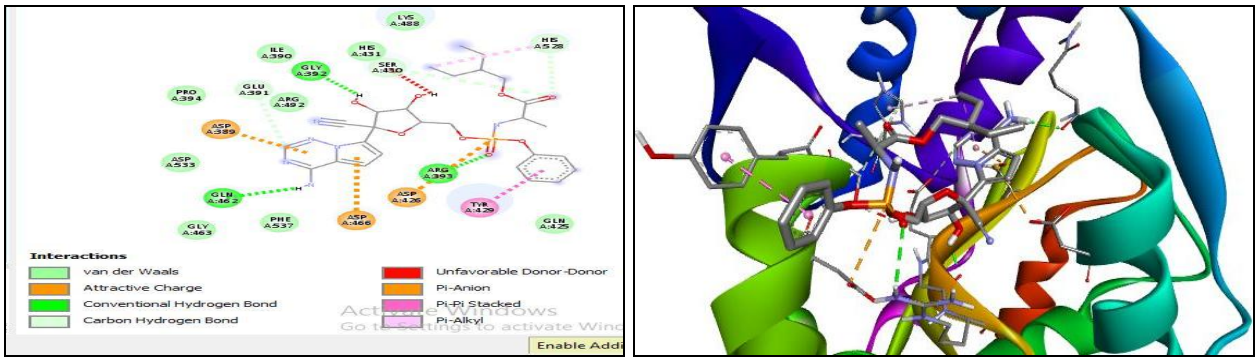

Ribavirin

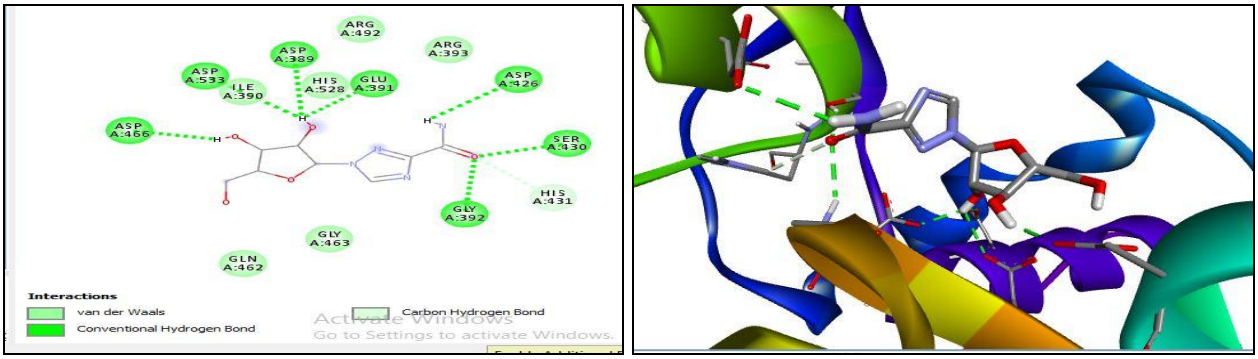

FIG. 8: THE BLIND DOCKED CONFORMATIONS OF INHIBITOR WITH 4GV9

ADME / Pharmacokinetic Predictions: Pharmacokinetic and toxic properties are imperative in drug safety assessment and also in the development of new drugs; these have made some drugs to be attrited at the trial stages and even for the approved drugs [42]. Poor pharmacokinetics, solubility, and bioavailability have been linked to low drug potency, toxicity, and drug failure [43, 44]. Therefore the prediction of ADMET properties are considered to be an important step in order to reduce possible challenges that may come up later at the clinical trial treatments. ADME (absorption, distribution, metabolism, and excretion) properties, as well as drug-likeness analysis, are considered for study in this work to help rationalizing the quality/failure of inhibitors/drugs administration to a biological system [45, 46]. The Pfizer's rule (Ro5) or Lipinski's rule of five (5) by Christopher A. Lipinski in 1997 is a thumb rule for evaluating drug-likeness and to decide if an inhibitor with acertain biological and pharmacological properties could be orally active drug in the human body 47. In the is work, ADMET properties were predicted using online tools pkCSM [48] and SwissADME 49 for two botanical drugs *(*Bergamottin and Casticin), and four synthetic drugs (Lacidipine, Phenothrine, Remdesvir, and Ribavirin) were evaluated for their pharmacokinetics and toxicity properties using *in-silico* approach. The rule states that a molecule or an inhibitor can be orally absorbed/active if two (2) or more of these thresholds; molecular weight (Mw) $\leq$ 500, octanol/water partition coefficient (iLOGP) $\leq$ 5, number of hydrogen bond acceptors (nHBA) $\leq$ 10, number of hydrogen bond donors (nHBD) $\leq$ 5, and topological polar surface area (TPSA) < 40 $Å^2$). The drug-likeness parameters are related to aqueous solubility and intestinal permeability, which determines the first step of oral bioavailability [50]. The drug-likeness prediction showed that Bergamottin, Casticin, Lacidipine and Ribavirin have zero violation of the Lipinski's rule except for Phenothrin and Remdesvir **Table 9.**

TABLE 9: DRUG LIKENESS OF THE LIGANDS

Drugs	Lipinski	Ghose	Veber	Egan	Muegge	Bioavailability score
Bergamottin	Yes	No	Yes	Yes	No	0.55
Casticin	Yes	Yes	Yes	Yes	Yes	0.55
Lacidipine	Yes	No	No	Yes	No	0.55
Phenothrine	Yes	No	Yes	Yes	No	0.55
Remdesvir	No	No	No	No	No	0.17
Ribavirin	Yes	No		No	Yes	).55

The drug-likeness parameters are related to aqueous solubility and intestinal permeability which determines the first step of oral bioavailability [51]. The results in **Table 10** also showed good pharmacokinetic properties in which Bergamottin, Casticin, Lacidipine and Phenothrin molecules have high gastrointestinal absorption while others have low GI absorption. P-gp inhibitors can affect or alter the pharmacokinetics properties of a drug [52], because P-gp molecules are present organs like BBB, bile ductule and kidney proximal tubule, so inhibition P-gp possibly increase the absorption, distribution, metabolism, and elimination of their substrates. Thus, it is very important to identify if a ligand is a substrate to Pgp *(i.e.* can be transported out of the cell) or inhibitor to Pgp (impair function). Lacidipine, Casticin and Remdesvir are predicted as both substrate, Bergamottin and Phenothrin as P-glycoprotein substrates and Ribavirin is neither P-glycoprotein substrate nor inhibitor.

Casticin, Lacidipine, Remdesvir, and Ribavirin possess blood-brain barrier BBB penetration except for Bergamottin and Phenothrin. The intestinal absorbance of the studied compounds is greater than 30%, indicating that all the combinations are highly absorbed through the intestine. However, Bergamottin, Casticin, Lacidipine and Phenothrin could be more absorbed than Remdesvir and Ribavirin Table 10. Therefore, Bergamottin and Casticin of botanical origin can be more absorbed easily be absorbed through the intestinal wall than Remdesvir and Ribavirin [53]. The Brain Or Intestinal Estimate D permeation predictive model (BOILED-Egg), also known as Egan egg graph of the drugs were generated from SwissADME online web server which revealed a clear graphical representation of the absorption of the molecules in the brain and gastrointestinal tract [48]. The graph molecules in the yolk area (yellow) are predicted to inactively permeate the blood-brain barrier (Bergamottin and Phenothrin), while Bergamottin,

Casticin, Lacidipine and Phenothrin are predicted to be highly absorbed in the gastrointestinal tract **Fig. 9**. These theoretical findings are in agreement with the experimentally pharmacokinetic profilereported [50].

Likewise, the bioavailability radar shows a rapid appraisal of the drug-likeness of a molecule by taking six (6) physicochemical properties into consideration: saturation, lipophilicity, polarity, size, solubility, and flexibility [51].

Fig. 10 shows the bioavailability radars of the drugs in which the molecules are predicted to be orally bioavailable (low flexibility and polarity), less toxic, and good absorption.

All the compounds are not toxic as predicted by AMES test, this is very crucial since the safety parameter is important to the development of a successful drug [52].

Inhibition of cytochrome P450 isoforms can lead to drug-drug interactions in which co-administered drugs fail to be metabolized, thereby can accumulate to toxic levels [54] some of the drugs can inhibit the cytochrome P450 isoforms with exception of Remdesvir and Ribavirin **Table 10.**

TABLE 10: ADMET PROFILE OF THE STUDIED DRUGS

Model							
Absorption (A)							
Water solubility	Numeric (Log moll/L)	-5.583	-6.433	-3.07	-1.712	--3.599	-5.26
Caco-2 permeability	Numeric (log Papp in 10^{-6} cm/s)	0.764	1.055	0.635	0.421	1.390	1.448
Skin permeability	Numeric (log Kp in cm/s)	-2.807	-2.506	-2.735	-2.763	-2.744	-2.55
Intestinal absorption (human)	Numeric (High/Low)	High/93.694	High/95.089	Low/71.109	Low/54.988	High/96.91	High/95.727
P-glycoprotein substrate	Categorical (Yes/No)	Yes	No	Yes	No	Yes	no
P-glycoprotein I Inhibitor		Yes	Yes	Yes	No	No	yes
P-glycoprotein II inhibitor		Yes	Yes	No	No	Yes	yes
Distribution (D)							
Blood-brain barrier (BBB)	Numeric (logBB)	No	No	Yes	Yes	No	yes
Metabolism (M)							
CYP1A2 inhibitor	Categorical (Yes/No)	Yes	No	No	No	Yes	Yes
CYP2C9 inhibitor		Yes	Yes	No	No	Yes	Yes
CYP2D6 inhibitor		Yes	Yes	No	No	No	No
CYP2C19 inhibitor		Yes	Yes	No	No	Yes	Yes
CYP3A4 inhibitor		Yes	Yes	Yes	No	Yes	Yes
Total Clearance	Numeric (log ml/min/kg)						
AMES toxicity	Categorical (Yes/No)	No	No	No	No	No	No
Synthetic accessibility	Numeric	4.86	3.89	6.33	3.89	3.71	3.72

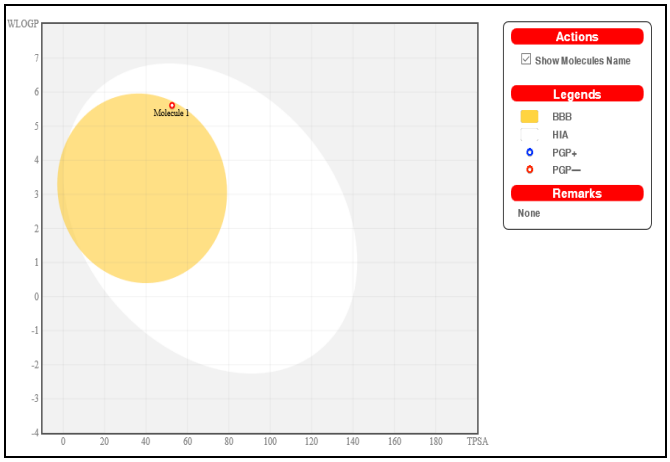

BERGAMOTTIN

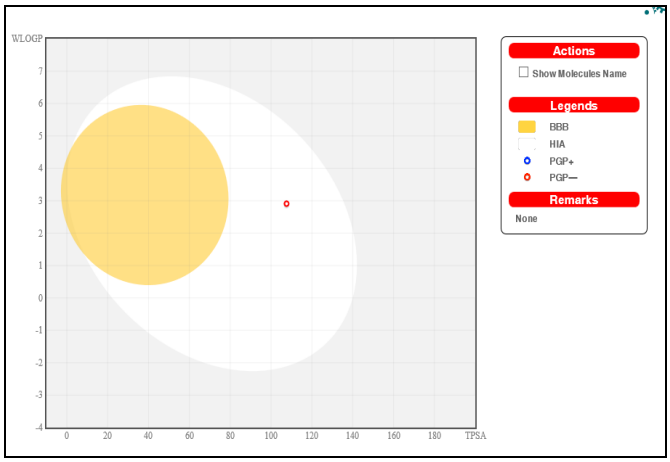

CASTICIN

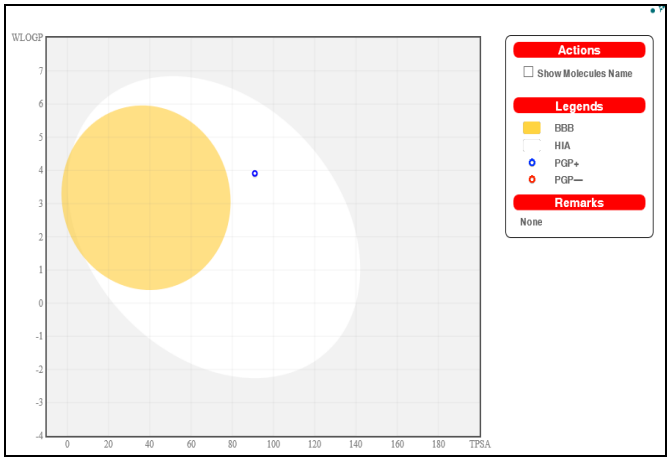

LACIDIPINE

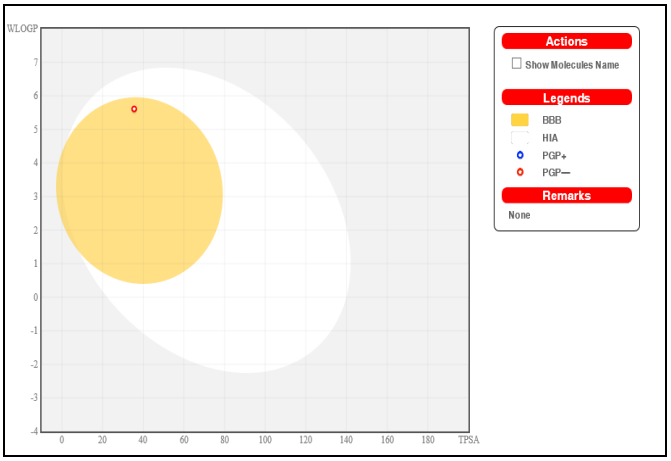

PHENOTHRIN

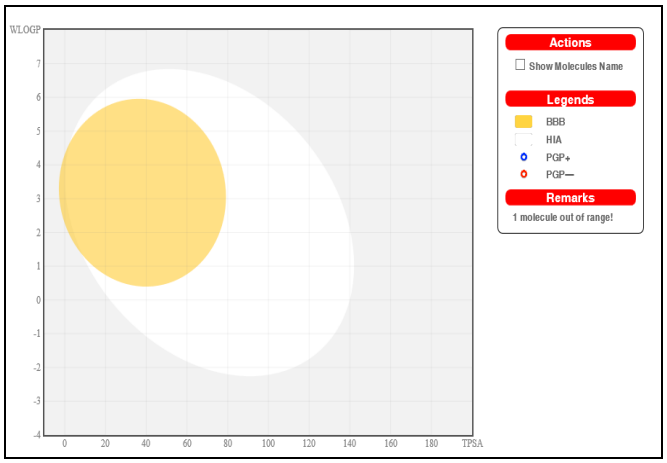

REMDESVIR

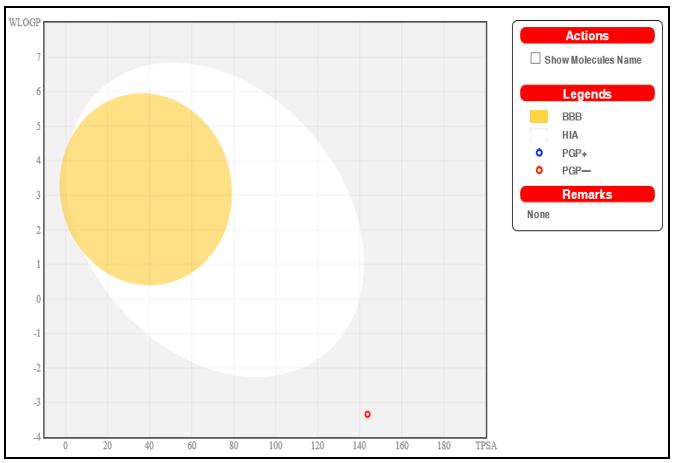

RIBAVIRIN

FIG. 9: BOILED-EGG GRAPH OF THE IPA MOLECULES

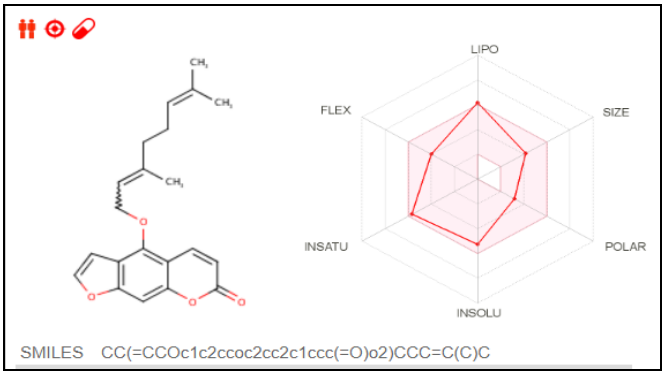

BERGAMOTTIN

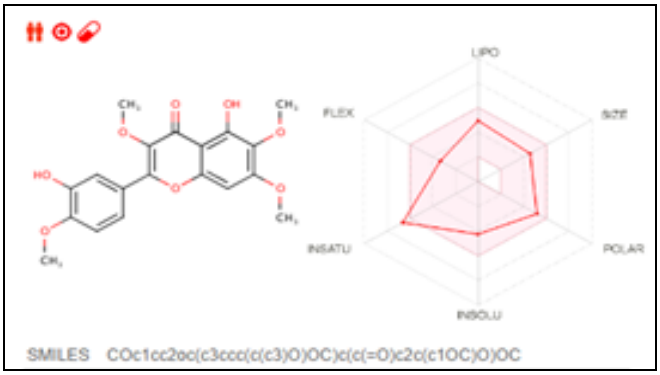

CASTICIN

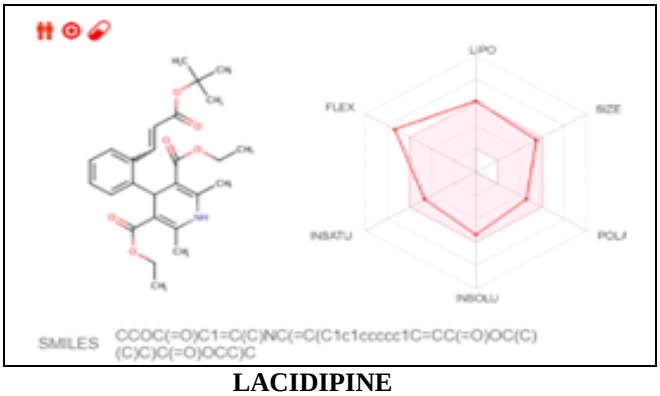

LACIDIPINE

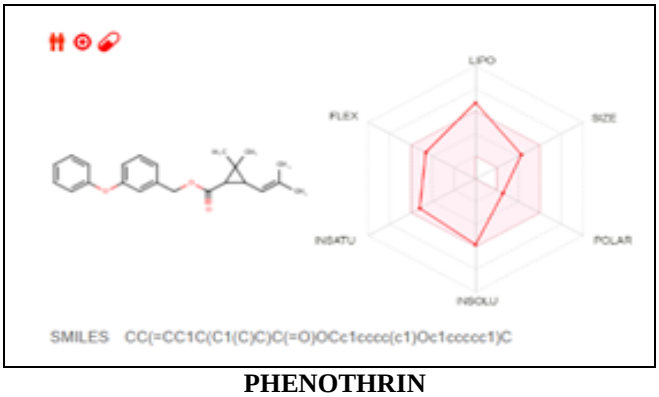

PHENOTHRIN

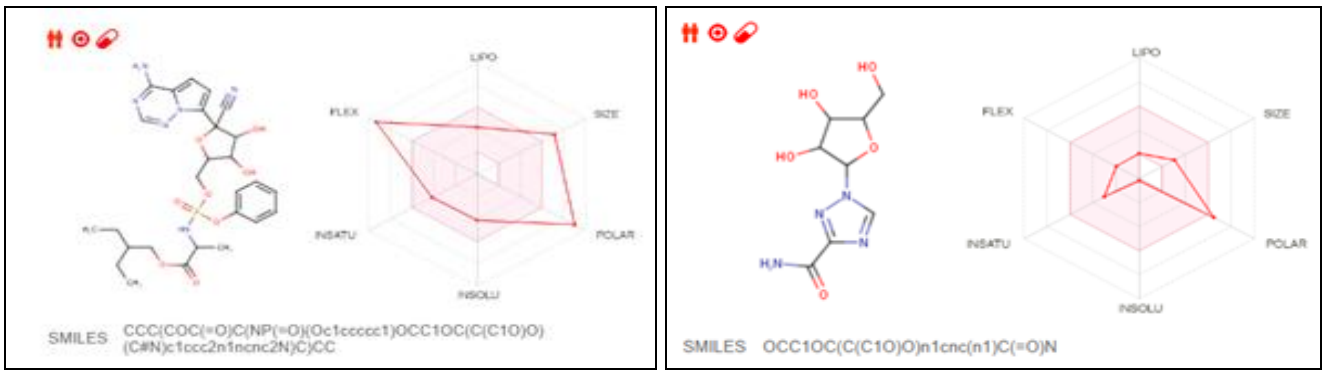

REMDESVIR **RIBAVIRIN**

FIG. 10: BIOAVAILABILITY RADAR OF THE BOTANICAL DRUGS (BERGAMOTTIN AND CASTICIN) AND COMMERCIALLY APPROVED DRUGS

CONCLUSION: The purpose of this study is to gauge the binding affinity of the botanical drugs (Casticin and Bergamottin) with some selected antiviral drugs ((Lacidipine, Phenothrine, Remdesvir and Ribavirin) being administered for the treatment of patients with Lassa fever.

The results showed that Remdesvir, Phenothrin and Casticin are more active against 3MWP; Remdesvir, Lacidipine and Casticin are active against 3MWT, 3MX5 and 3T5Q; Remdesvir, Bergamottin and Casticin against 3T5N; Remdesvir, Casticin and Bergamottin showed more inhibitory action against 4FVU. Generally, Remdesvir showed outstanding inhibitory action against nucleoprotein (NP) of the Lassa virus, NP for the RNA synthesis and immune suppression, NP for the genomic ribonucloeprotein complexes, NP exonuclease activity causes suppression of innate immune signaling the infected cell, and 3'-5' exoribonuclease suppresses type 1 interferon (IFN).

Also Casticin, a botanical drug showed very good activity against a number of nucleoproteins (NP) of the Lassa virus than Bergamottin, thus could be used to treat Lassa fever. ADMET profile revealed that Bergamottin, Casticin, Lacidipine and Phenothrin could be readily absorbed than Remdesvir and Ribavirin into intestinal wall; therefore, Bergamottin and Casticin of botanical origin can easily be absorbed through intestinal wall than Remdesvir and Ribavirin. All the drugs can inhibit the cytochrome P450 isoformsin except Remdesvir and Ribavirin.

Research Funding: The authors received no funding for this work.

ACKNOWLEDGEMENT: The authors are grateful to the Department of Pure and Applied Chemistry for the computational resources

CONFLICT OF INTEREST: The authors have no conflict of interest.

REFERENCES:

1. Paolo Colangelo EV, Leirs H, Tatard C, Denys C, Dobigny G, Duplantier JM, Brouat C, Granjon L and Lecompte E: A mitochondrial phylogeographic scenario for the most widespread African rodent, Mastomys natalensis. Biological Journal of the Linnean Society 2013; 108: 901–916.
2. Olayemi A, Cadar D, Magassouba N, Obadare A, Kourouma F, Oyeyiola A, Fasogbon S, Igbokwe J, Rieger T and Bockholt S: New Hosts of the Lassa Virus Sci Rep 2016: 6: 25280.
3. Childs JE, Mills JN and Glass GE: Rodent-Borne Hemorrhagic-Fever Viruses A Special Risk for Mammalogists. J Mammal 1995; 76: 664–680.
4. Greenky D, Knust B and Dziuban EJ: What Pediatricians Should Know About Lassa Virus. JAMA Pediatrics 2018; 172: 407–408.
5. Richmond JK and Baglole DJ: Lassa fever: Epidemiology, clinical features, and social consequences". BMJ 2003; 327:1271–1275.
6. "Lassa fever situation report" (PDF). Nigeria Centre for Disease Control Protecting the health of Nigerians.March 2020 (www.ncdc.gov.ng)
7. Centers for Disease Control and Prevention, "Lassa Fever, Signs and Symptoms"Archived 9 July 2017 at the Wayback MachineLassa Fever: https://www.cdc.gov/vhf/lassa/index.html (accessed on 1 January 2020).
8. Content source: Centers for Disease Control and Prevention, National Center for Emerging and Zoonotic Infectious Diseases (NCEZID), Division of High-Consequence Pathogens and Pathology (DHCPP), Viral Special Pathogens Branch (VSPB). U.S. Department of Health & Human Services. https://www.cdc.gov/vhf/lassa/symptoms/index.html (March 25, 2014)
9. Childs JE, Mills JN and Glass GE: Rodent-Borne Hemorrhagic-Fever Viruses A Special Risk for Mammalogists. J Mammal 1995; 76: 664–680.

10. Wang P, Liu Y, Zhang G, Wang S, Guo J, Cao J, Jia X, Zhang L, Xiao G and Wang W: Screening and identification of lassa virus entry inhibitors from an FDA-Approved library. Journal of Virology 2018; 92: 00954-18. Doi: 10.1128/jvi.00954-18
11. Audray D-J, Alexandre O, Alain H, Gilles C, Ollitrault O, Yann F and Frédéric B: The Distribution of Coumarins and Furanocoumarins in Citrus Species Closely Matches Citrus Phylogeny and Reflects the Organization of Biosynthetic Pathways". PLoS One 2015; 10: 0142757.
12. Wang P, Liu Y, Zhang G, Wang S, Guo J, Cao J, Jia X, Zhang L, Xiao G and Wang W: Screening and identification of Lassa virus entry inhibitors from an FDA-approved drug library. J Virol 2018; 92: 00954-18. doi:10.1128/JVI.00954-18.
13. Eva H, Beat M and Otto S: "An analytical high performance liquid chromatographic method for the determination of agnuside and p-hydroxybenzoic acid contents in Agni-casti fructus". Phytochemical Analysis 2000; 11: 327–329. doi:10.1002/1099-1565
14. Liu Y, Guo J, Cao J, Zhang G, Jia X, Wang P, Xiao G and Wang W: Screening of botanical drugs against Lassa virus entry. J Virol 2021; 95: 02429-20. https://doi.org/10.1128/JVI.02429-20.
15. Eichler R, Lenz O, Strecker T and Garten W: Signal peptide of Lassa virus glycoprotein GP-C exhibits an unusual length. FEBS Lett 2003; 538: 203–206. https://doi.org/10.1016/s0014-5793(03)00160-1.
16. Shankar S, Whitby LR, Casquilho-Gray HE, York J, Boger DL and Nunberg JH: Small-molecule fusion inhibitors bind the pH-sensing stable signal peptide-GP2 subunit interface of the Lassa virus envelope glycoprotein. J Virol 2016; 90: 6799–07. https://doi.org/10.1128/JVI.00597-16.
17. Wang P, Liu Y, Zhang G, Wang S, Guo J, Cao J, Jia X, Zhang L, Xiao G and Wang W: Screening and identification of Lassa virus entry inhibitors from an FDA-approved drug library. J Virol 2018; 92: 00954-18. https://doi.org/10.1128/JVI.00954-18.
18. Tang K, Zhang X and Guo Y: Identification of the dietary supplement capsaicin as an inhibitor of Lassa virus entry. Acta Pharm Sin B 2020; 10: 789–798.https://doi.org/10.1016/j.apsb.2020.02.014.
19. Newman DJ and Cragg GM:, Natural products as sources of new drugs over the nearly four decades from 01/1981 to 09/2019. J Nat Prod 2020; 83: 770–803. https://doi.org/10.1021/acs.jnatprod.9b01285.
20. Qi X, Lan S, Wang W, Schelde LM, Dong H, Wallat GD, Ly H, Liang Y and Dong C: Cap binding and immune evasion revealed by Lassa nucleoprotein structure. Nature 2010; 468: 779-783.
21. Hastie KM, Liu T, Li S, King LB, Ngo N, Zandonatti MA, Woods VL, de la Torre JC and Saphire EO: Crystal structure of the Lassa virus nucleoprotein-RNA complex reveals a gating mechanism for RNA binding. Proc Natl Acad Sci U S A 2011; 108: 19365-19370.
22. Hastie KM, King LB, Zandonatti MA and Saphire EO: Structural Basis for the dsRNA Specificity of the Lassa Virus NP Exonuclease. PLoS One 2012; 7: 44211-44211.
23. Jiang X, Huang Q, Wang W, Dong H, Ly H, Liang Y and Dong C: Structures of Arenaviral Nucleoproteins with Triphosphate dsRNA reveal a Unique Mechanism of Immune Suppression. J Biol Chem 2013; 288: 16949-16959.
24. Spartan user's guide, Wave function, Inc, Irvine, CA 92612 USA 2014
25. Hehre WJ, Radom L, Schleyer PVR and Pope JA: Ab initio molecular Orbital Theory. Wiley New York 1988.
26. Becke AD: Density-functional thermochemistry. III. The role of exact exchange. Journal Chemical Physics 1993; 98: 5648-5652. DOI: 10.1063/1.464913
27. Lee C, Yang W and Parr RG: Development of the Colle-Salvetti correlation-energy formula into a functional of the electron density. Physical Review B: 1988; 37: 785-789. DOI: 10.1103/physrevb.37.785
28. Spartan'14 Wavefunction, Inc. Irvine, CA, 2014
29. Trott O and Olson AJ: AutoDockVina: improving the speed and accuracy of docking with a new scoring function, efficient optimization and multithreading. J Comput Chem 2010; 31: 455–461.
30. Adegbola PI, Semire B, Fadahunsi OS and Adegoke AE: Molecular docking and ADMET studies of Allium cepa, *Azadirachta indica* and Xylopia aethiopica isolates as potentialanti-viral drugs for Covid-19. Virus Dis 2021; https://doi.org/10.1007/s13337-021-00682-7
31. Oyebamiji AK, Tolufashe GF and Semire B: Inhibition study on anti-type 3 of 3α-hydroxysteroid dehydrogenase activity against 1, 2, 3-triazolo[4,5-D] pyrimidine derivatives: Molecular modelling approach. Scientific African 2020; 8: 00444.
32. Oyebamiji AK, Oladipo EK, Olotu TM, Awoyelu HE, Adamolekun E and Semire B: *In-vitro* Investigation on Selected 32compounds in Annona Muricata Seed: A Potential SARS-CoV nsp12 Polymerase Inhibitors down Regulating 2019-nCoV. Int J Tradit Nat Med 2020; 10: 13-23.
33. Oyebamiji AK, Fadare OA and Semire B: Hybrid-based drug design of 1,2,3-triazolepyrimidine-hybrid derivatives: Efficient inhibiting agents of mesenchymal–epithelial transition factor reducing gastric cancer cell growth. J. Chem Res 2020; 44: 277-280: doi.org/ 10.1177/1747519819898354
34. Oyewole RO, Oyebamiji AK and Semire B: Theoretical Calculations of Molecular Descriptors for Anticancer Activities of 1,2,3- Triazole-pyrimidine derivatives against Gastric cancer cell (MGC-803): DFT, QSAR and Docking Approaches. Heliyon 2020; 6: 03926 doi.org/10.1016/j.heliyon.2020.e03926
35. Adegbola AE, Fadahunsi OS, Ayodeji AA, Abijo Z, Balogun TA, Aderibigbe TS, Semire B and Adegbola PI: Computational prediction of nimbanal as potential antagonist of respiratory syndrome coronavirus. Informatics in Medicine Unlocked 2021; 24: 100617 https://doi.org/10.1016/j.imu.2021.100617
36. Adegbola PI, Fadahunsi OS, Adegbola AE and Semire B: *In-silico* studies of Potency and safety assessment of selected trial drugs for the treatment of COVID 19. In Silico Pharmacology 2011; 9: 45 https://doi.org/10.1007/s40203-021-00105-x
37. Oyebamiji AK, Akintelu SA, Amao OP, Kaka MO, Morakinyo AE, Amao FA and Semire B: Dataset on Theoretical Bio-Evaluation of 1,2,4-Thiadiazole-1,2,4-Triazole Analogues against Epidermal Growth Factor Receptor Kinase down Regulating Human Lung Cancer. Data in Brief 2021; 37: 107234.
38. Nasution MAF, Toepak EP, Alkaff AH and Tambunan US: Flexible docking-based molecular dynamics simulation of natural product compounds and Ebola virus Nucleocapsid (EBOV NP): a computational approach to discover new drug for combating Ebola. BMC Bioinformatics 2018; 19(14): 419. DOI: 10.1186/s12859-018-2387-8
39. Antonius Y, Ongko J, Sukweenadhi J and Dwi Putra SE: Identification of Potential Ebola Virus Nucleoprotein (EBOV NP) Inhibitor Derivate from Various Traditional

Medicinal Plants in Indonesia: *in-silico* study. Media Pharmaceutica Indonesiana 2021; 3: 217-2261.
40. Wass MN, Kelley LA and Sternberg MJE: 3DLigand Site: predicting ligand-binding sites using similar structures. Nucleic Acids Research 2010; 38: 469–473.
41. Ferreira LG, dos Santos RN, Oliva G and Andricopulo AD: Molecular docking and structure-based drug design strategies. Molecules 2015; 20: 13384-13421.
42. Waring MJ, Arrowsmith J, Leach AR, Leeson PD, Mandrell S and Owen RM: An analysis of the attrition of drug candidates from four major pharmaceutical companies. Nat Rev Drug Discov 2015; 14: 475–86.
43. Sadgrove NJ and Jones GL: From Petri Dish to Patient: Bioavailability Estimation and Mechanism of Action for Antimicrobial and Immunomodulatory Natural Products Front Microbiol 2019; 10: 2470.
44. Darvas F, Keseru G, Papp A, Dorman G, Urge L and Krajcsi P: *In-silico* and Exsilico ADME approaches for drug discovery. Top Med Chem 2002; 2: 1287–304.
45. Attique SA, Hassan M, Usman M, Atif RM, Mahboob S, Al-Ghanim KA, Bilal M and Nawaz MZ: A molecular dock-ing approach to evaluate the pharmacological properties of natu-ral and synthetic treatment candidates for use against hyperten-sion. Int J Environ Res Public Health 2019; 16(923): 1–17. https://doi.org/10.3390/ijerph16060923
46. Umar AB, Uzairu A, Shallangwa, GA and Uba S, Design of potential anti-melanoma agents against SK-MEL-5 cell line using QSAR modeling and molecular docking methods. SN Appl Sci 2020; 2: 815.
47. PiresDEV, BlundellTL and AscherDB, pkCSM: predicting small-molecule pharmacokinetic and toxicity properties using graph-based signatures. J Med Chem 2015; 58: 4066–4072.
48. Daina A, Michielin O and Zoete V: SwissADME: a free web tool to evaluate pharmacokinetics, drug-likeness and medicinal chemistry friendliness of small molecules. Sci Rep 2017; 7: 42717.
49. Cheng X, Li P, Chen Z, Zhang N, Zhen Y, Zhao L, Wang X and Wu R: Break-through bleeding in relation to pharmacokinetics of factor VIII in paediatric patients with severe haemophilia A. Haemophilia 2018; 24: 120–125. doi: 10.1111/hae.13373
50. Daina A and Zoete V: A boiled-egg to predict gastrointestinal absorption and brain penetration of small molecules 2016; 1117–1121. https://doi.org/10.1002/cmdc.201600182
51. Amin ML: P-glycoprotein inhibition for optimal drug delivery. Drug Target Insights 2013; 7: 27–34.
52. Wang A, Lv K, Li L, Liu H, Tao Z, Wang B, Liu M, Ma C, Ma X, Han B, Wang A and Lu Y: Design, synthesis and biological activity of N-(2-phenoxy) ethyl imidazo [1,2-a]pyridine-3-carboxamides as new antitubercular agents. Eur J Med Chem 2019; 178: 715–725.
53. Hadni H and Elhallaoui M: 3D-QSAR, docking and ADMET properties of aurone analogues as antimalarial agents, Heliyon 2020; 6: 03580.
54. Lynch T and Price A: The effect of cytochrome P450 metabolism on drug response, interactions, and adverse effects. Am Fam Physician 2007; 76: 391–396.

How to cite this article:
Omotayo IA, John AA, Gbenga OO, Misbaudeen A, Felix LD, Kolawole OA and Banjo S: *In-silico* assessment via molecular docking and admet profile of botanical drugs (Bergamottin and Casticin) against trial drugs for lassa virus. Int J Pharm Sci & Res 2022; 13(9): 3494-18. doi: 10.13040/IJPSR.0975-8232.13(9).3494-18.